DEVELOPMENT OF MONOLITHIC CERAMICS AND HIGH-TEMPERATURE COATINGS

Kennametal's Hot-Section Materials Development

R. Yeckley, J. R. Hellmann, K. M. Fox, D. J. Green, and E. C. Dickey
Kennametal Inc.
1600 Technology Way, P.O. Box 231, Latrobe, PA 156-0231
Phone: (724) 539-4822, E-mail: Russ.yeckley@kennametal.com

Objective

Determine potential of an existing structural SiAlON that is being manufactured for other applications that, commensurate with the requirements of advanced microturbines shows potential for strength, environmental stability, and manufacturability for complex shapes.

Highlights

Keiser rig tests are completed for two SiAlONs from the screening matrix. Both SiAlONs have the higher rare earth content. SiAlON ab832 performed poorly. The second SiAlON ab532 is comparable to silicon nitrides previously tested.

Technical Progress

Two SiAlONs from the screening matrix were sent to K. More at ORNL for corrosion testing in the Keiser Rig. The two SiAlONs are ab532 and ab832. Both have the higher rare earth content. The mechanical properties for these SiAlON are shown in Table 1. Samples from each SiAlON were run at 1200 C, 3 % H_2O and 1200 C with 20% H_2O. The SiAlON behaviors are quite different. SiAlON ab832 has a very high corrosion rate. SiAlON ab532's corrosion behavior is very similar to other silicon nitrides tested. The corrosion resistance may be related to the SiAlON solid solution. SiAlON ab532 with the better corrosion resistance and has greater substitution of Al, O in the β SiAlON and α SiAlON crystal structures. Weight loss and reaction layer thickness after 2000 hours are summarized Figure 1 and Figure 2 for the two SiAlONs. Weight loss with time is plotted in Figure 3 for ab532. Morphology of the corrosion layer is very similar to silicon nitride. The corrosion mechanism in water vapor appears to be the same for SiAlON as silicon nitride. Figures 4-7 are SEM photos depicting the corrosion layer observed on SiAlON ab532.

Table 1 SiAlON Properties

Composition ID	ab832	ab532
Hardness (GPa)	18.72±0.35	17.38±0.58
Fracture Toughness, K_{1C} (MPa√m)	7.36±0.22	5.73±0.16
Fracture Strength (MPa) at RT	783	651
Weibull Modulus at RT	6.06	5.92
Fracture Strength (MPa) 1204°C	540	393
Weibull Modulus at 1204°C	6.25	9.75
α-SiAlON Content (w/o)	44	35.8
α-SiAlON x'	0.248	0.40
ß-SiAlON z'	0.376	0.820

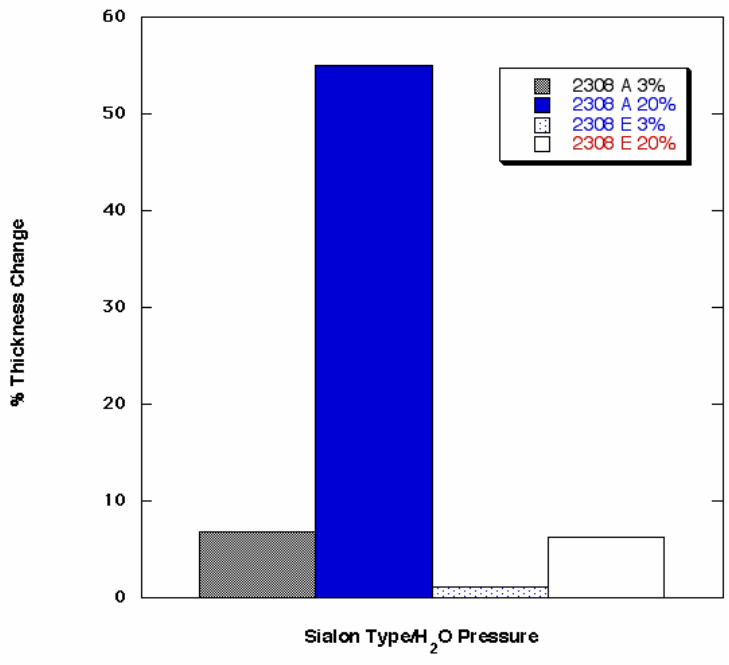

Figure 1. Thickness change after 2000 hours in Keiser Rig. In the legend, 2308A is ab832 and 2308E is ab532.

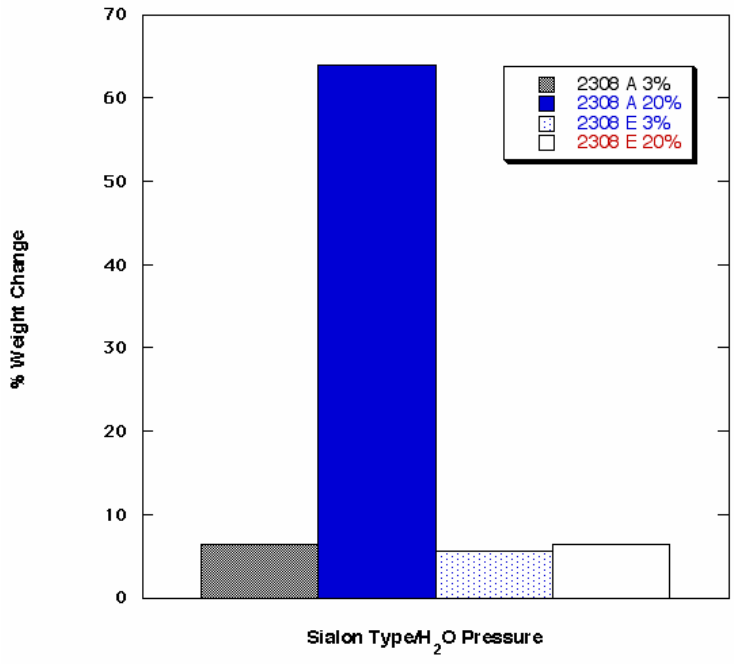

Figure 2. Weight change after 2000 hours in the Keiser Rig. In the legend, 2308A is ab832 and 2308E is ab532.

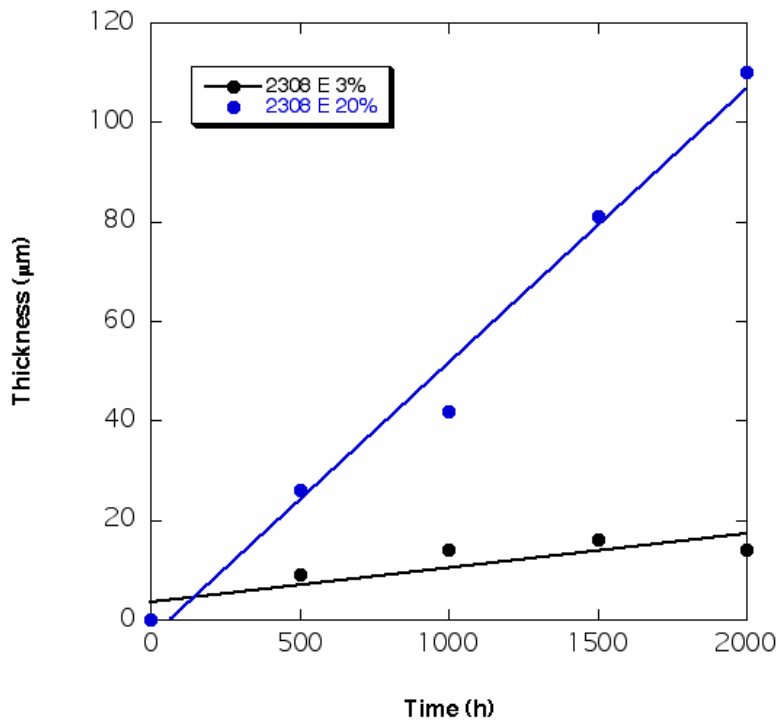

Figure 3. Thickness change with time for SiAlON ab532.

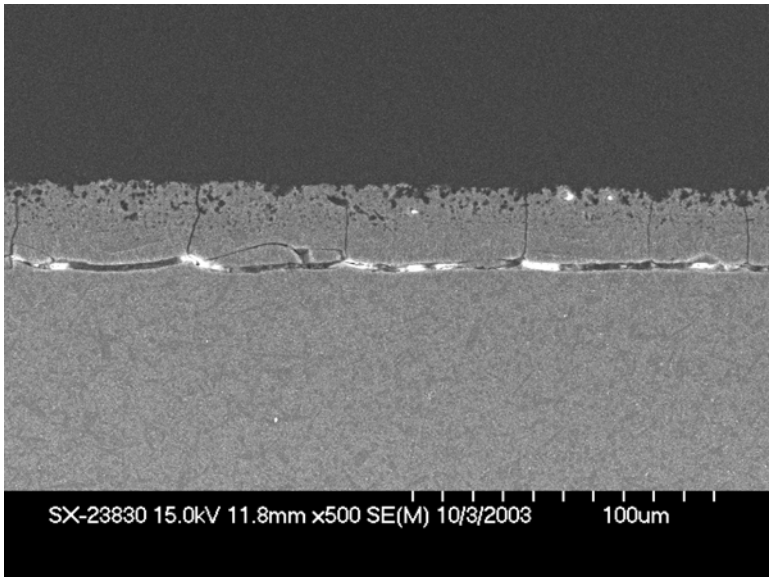

Figure 4. SEM micrograph showing corrosion layer after 500 hours in 20% water vapor for SiAlON ab532.

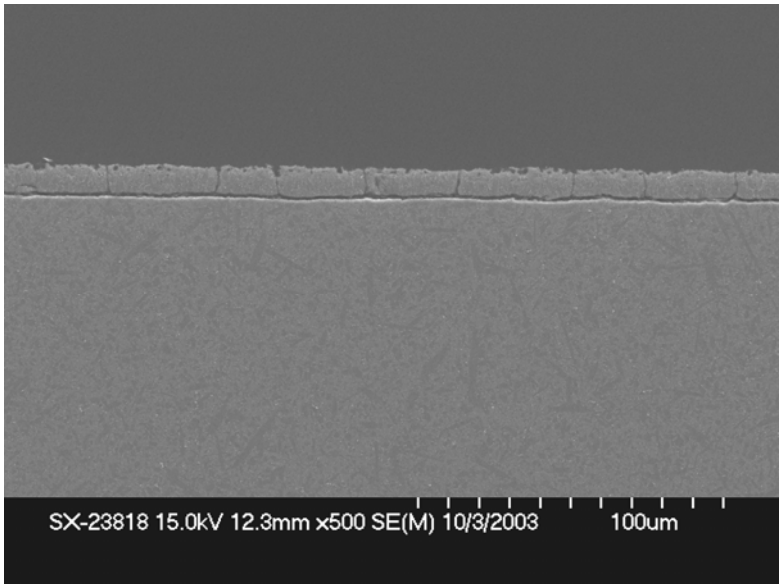

Figure 5. SEM micrograph showing corrosion layer after 500 hours in 3% water vapor for SiAlON ab532.

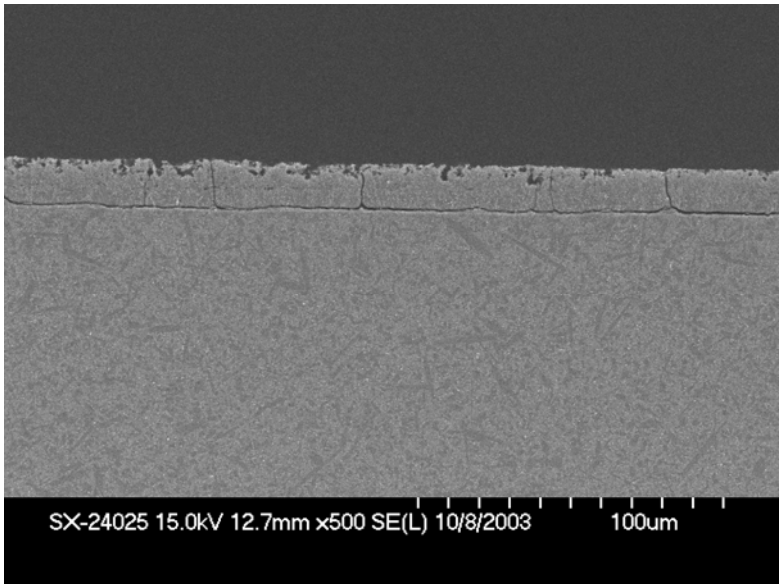

Figure 6. SEM micrograph showing corrosion layer after 1500 hours in 3% water vapor for SiAlON ab532.

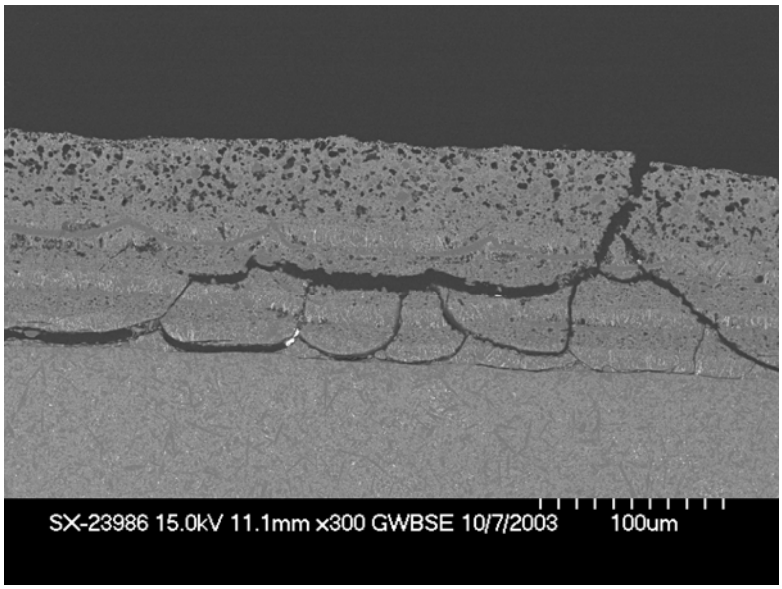

Figure 7. SEM micrograph showing corrosion layer after 1500 hours in 20% water vapor for SiAlON ab532.

Completion of the Keiser rig testing ends the work with the SiAlON screen matrix. SiAlON ab532 demonstrated that SiAlON could equal the corrosion performance of silicon nitride. Additional testing will be conducted on SiAlONs containing less rare earth additive.

Two SiAlONs from the matrix are selected for additional mechanical testing and environmental testing. The SiAlONs are ab831and ab531. These SiAlONs contain 30% less rare earth than the SiAlONs tested in the Keiser rig. Four tile of each SiAlON were sent for Keiser rig testing. Also, tiles are completed for flexure bar preparation. Strengths will be determined for the machined surface and as processed surface. Tensile rod blanks are completed and sintering will be completed in June.

The SiAlONs prepared in the screening matrix have β SiAlON z values ranging from 0.3 to 0.8. A similar range in β SiAlON z value exists between the two SiAlONs selected for continued evaluation. The SiAlON microstructure characteristics are similar at equivalent z values. The β SiAlON grains have a lower aspect ratio at higher z values. SEM images showed lower grain boundary volume with higher z SiAlONs. The grain boundaries were analyzed by TEM to determine whether a grain boundary film is present. The high z SiAlON ab582 has a high percentage of grain boundaries with no apparent amorphous film. A grain boundary is shown in Figure 8 with no amorphous film.

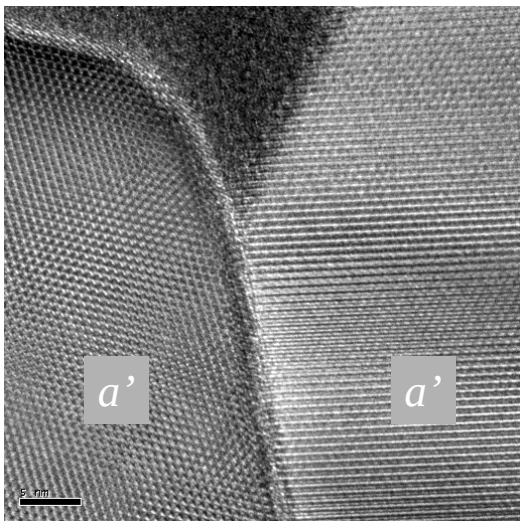

Figure 8. A grain boundary between α SiAlON grains. No amorphous film is apparent.

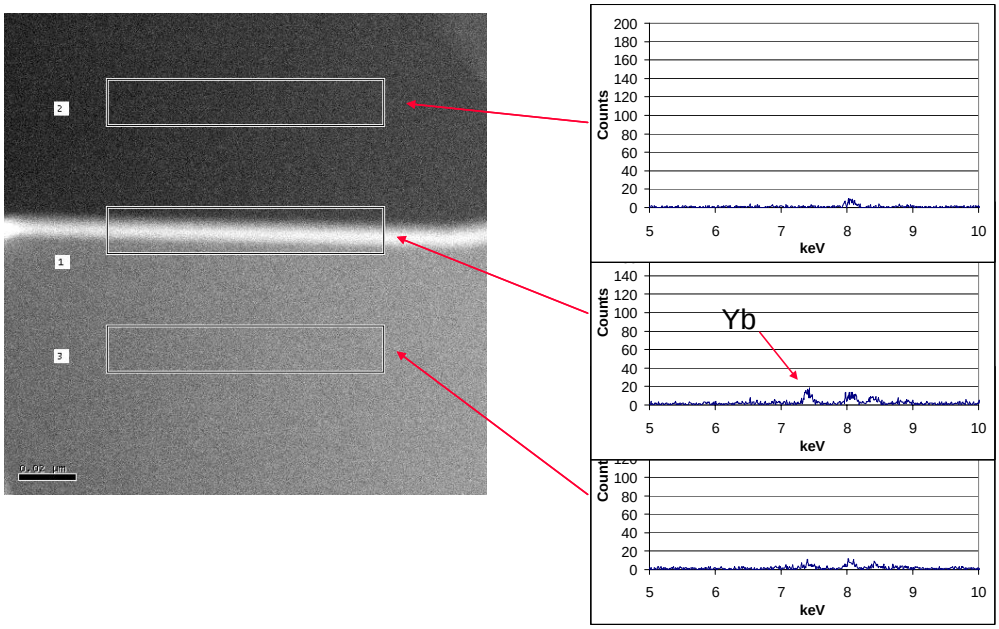

Figure 9. Amorphous film present in grain boundary between a β SiAlON and α SiAlON grain. Higher Yb is present in the grain boundary.

Many grain boundaries in the low z SiAlON, ab831, have a amorphous phase present as shown in Figure 9. Also grain boundaries with no amorphous phase were observed in ab831. Figure 10 is a grain boundary between α SiAlON grains. Figure 11 is a grain boundary between β SiAlON grains. EDS did not detect the presence of the rare earth at the grain boundary. The difference in Keiser Rig performance could be influenced by the grain boundary structure.

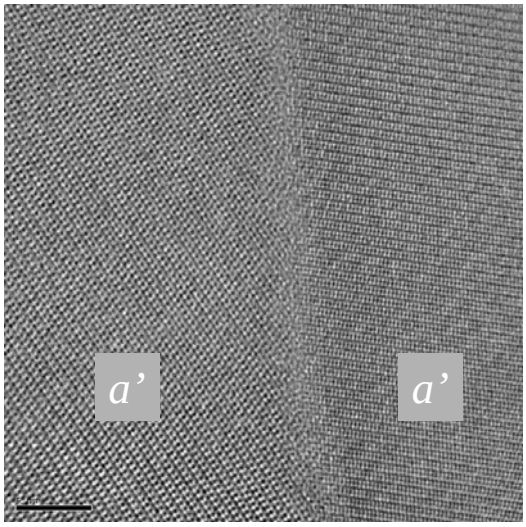

Figure 10. Grain boundary in SiAlON ab831.

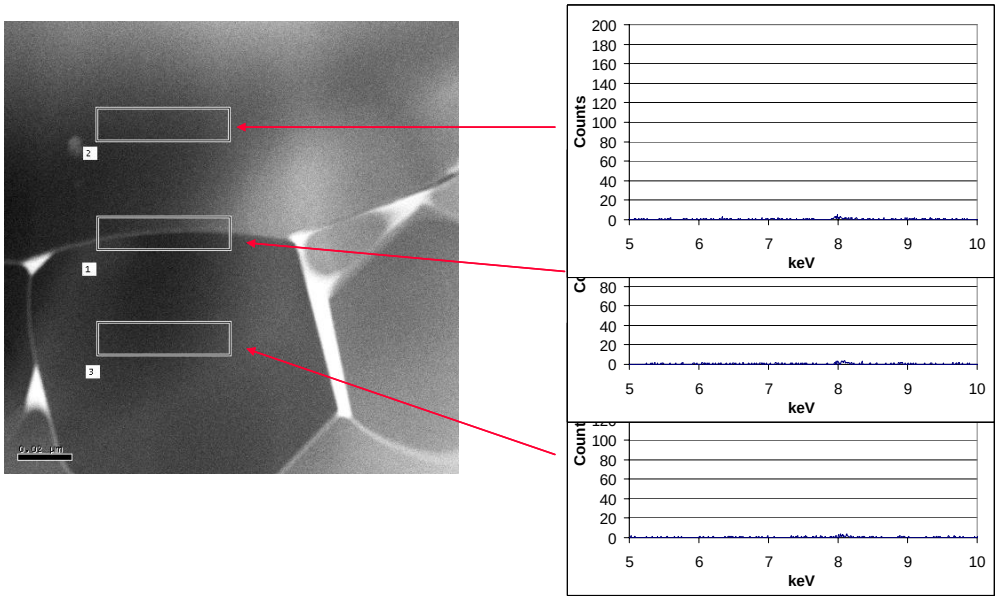

Figure 11. Grain boundary between β SiAlON grains. No Yb is observed at the interface suggesting there is not an amorphous film present.

The results from the first four hertzian creep tests are in Figure 12. The indenter is a 2mm diameter SiC cylinder. Profilometer trace of the impression shows that excellent alignment is achieved between the indenter and specimen surface. The creep tests are conducted on polished SiAlON surfaces. The creep rate differences between the two SiAlONs are interesting. SiAlON ab582 has 57 % α SiAlON and a small volume of grain boundary phase. SiAlON ab831 contains 31% α SiAlON and more grain boundary but exhibits lower creep. SiAlON ab582 microstructure is more equiaxed than ab831. SiAlON ab582 has a fracture toughness of 4.9 MPa $m^{1/2}$ compared to 6.9 MPa $m^{1/2}$ for ab831. The ab582's equiaxed structure may allow a greater grain boundary-sliding rate than ab831.

Temperature and stress will be varied in future creep experiments. ORNL provided NT154 for hertz creep testing as a comparison to the SiAlON. Also, ORNL will measure compressive creep of the SiAlONs for comparison with the hertzian creep tests.

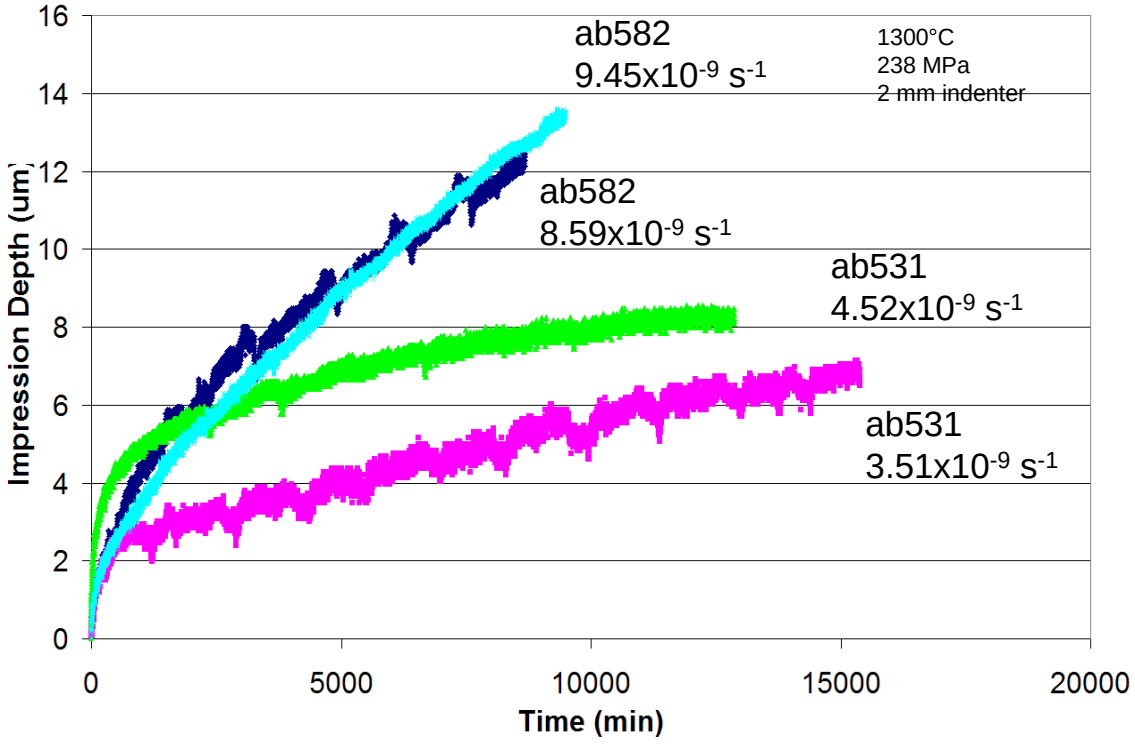

Figure 12. Deformations with time for the hertzian creep tests.

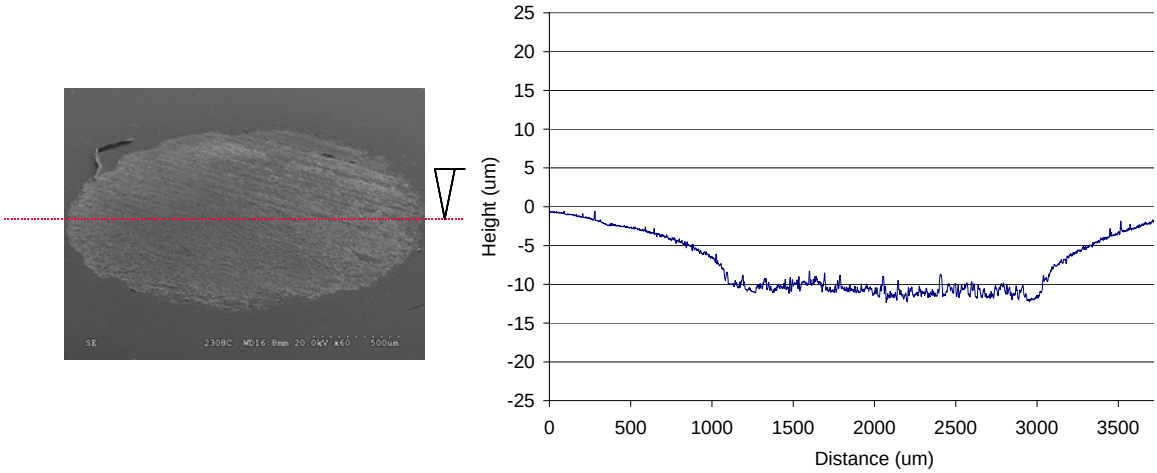

Figure 13. Excellent alignment is attained during creep tests as shown by the profilometer trace of the impression.

Status of Milestones

1) SiAlON compositional preliminary matrix - completed
2) Complete mechanical and microstructural characterization of initial SiAlON compositions.

Sept ‘04

a. Prepare flexure bars (ground and as processed surface) – Densification complete. Flexure bar finishing in process.
b. Tile for Keiser Rig testing – complete, sent to ORNL
c. Deliver tensile rods to ORNL – Densification scheduled for completion in June.

3) Colloidal Processing of Silicon Nitride Apr. ‘04

On schedule for completion in April. Final report and process transfer to Kennametal will occur in June.

4) Role of Microstructure and Crystalline Phase Evolution on Thermo-mechanical Properties of SiAlON Ceramics for Microturbine Applications Oct. ‘04

This effort is on schedule.

Problems Encountered

None

Publications/Presentations

Presented at the Amer. Cer. Society Annual Meeting: “Role of microstructure and crystalline phase evolution on thermomechanical properties of SiAlON ceramics for microturbine applications.” K. Fox, Prof. J Hellman and R Yeckley

Saint-Gobain Hot -Section Materials Development

R. H. Licht, Vimal K. Pujari, William T. Collins, James M. Garrett, Ara M. Vartabedian
Saint-Gobain Ceramics & Plastics, Inc.
Goodard Road, Northboro, MA 01532
Phone: (508) 351-7815, E-mail: Robert.h.licht@saint-gobain.com

Objective

The goal of this program is to develop and optimize a high temperature silicon nitride based ceramic material and process suitable for microturbine hot section component applications.

Highlights

The technical effort during this reporting period focused on a) the optimization of As-Processed (AP) surfaced properties of NT154 (PHASE 1) and b) to launch PHASE II program with activity leading to a recession resistant NT154 material and net-shape components.

Utilizing the proprietary new HIP process reported previously, the targeted AP strength of 700MPa was reproduced in the production HIP.

The Phase II effort to develop a robust solution for the "recession" of silicon nitride, in the gas turbine environment, was also launched. More specifically, the technical approach focused on two techniques to modify the silicon nitride surface. Namely, HEEPS (Hip Engineered Environmental Protection System) and Pack Cementation.

Technical Progress

The technical effort involves a two-pronged approach:

1. Material development
2. Net Shape Forming Development (NSFD)

1. MATERIAL DEVELOPMENT:

1.1 AP Strength Optimization

Optimization of the as-processed (AP) surface strength of NT154 using a larger, production HIP continued this period. As has been reported previously, a new proprietary HIP process, has been shown to reduce the reaction layer and the surface roughness of the dense NT154. The target AP strength of 700MPa, as reported previously using a smaller, laboratory-scale HIP furnace, has been duplicated in the production HIP. An excellent AP Strength of 717MPa was achieved. Based on the work to date, the desired conditions leading to target AP strength have been identified. We are working towards consistently reproducing the target AP strength.

1.2 Recession Mitigation

Material recession, due to volatilization in humid gas turbine environments, is an issue for silicon nitride and has been reported on in the literature. Phase II of the contract investigates recession resistant solutions for NT154. Two different approaches are currently being investigated internally:

a) HEEPS - HIP Engineered Environmental Protection Surface
b) Pack Cementation

1.2.1 HEEPS

Under the HEEPS approach, pre-sintered NT154 tiles were surface modified / dip coated with various suitable recession resistant compounds. Based on microprobe and micro-XRD analyses, the surface was not adequately modified. Some experiments are planned in an attempt to minimize the coating material migration and help develop the desired surface modification deemed to be suitable under a humid oxidative environment.

1.2.2 Pack Cementation

Some initial, scoping pack cementation experiments are underway. Dense NT154 tiles with AP and machined surfaces were embedding in various rare earth oxides at various temperatures and gaseous environments. SEM, EDS, and XRD were performed to characterize the modified surface layers. The analyses indicate the formation of rare-earth silicates up to depths of 8 m. Unfortunately, the rare-earth silicates have not formed a continuous layer to protect the base silicon nitride. Several pack cementation experiments are planned to investigate several parameters (time, temperature, environment, and powder bed). The goal is to change the surface of the silicon nitride to a continuous rare-earth silicate layer with sufficient depth. Pack cementation samples, along with the HEEPS specimens mentioned above, are being recession tested using a simplified screening test procedure developed at NRDC as described below.

Collaboration in this area, with Steve Nunn at ORNL, is also planned.

1.2.3 Recession Screening Test

A simple recession screening test has been developed at Northboro Research and Development Center (NRDC). The test will allow us to down select techniques and process parameters for further optimization. Suitable candidates will then be delivered to Karren More at ORNL for Keiser Rig Testing.

In the NRDC test, a controlled amount of humidified air is allowed to flow through a tube furnace which is maintained at a desired temperature. The test allows capability to control the $\%H_2O$ in the air, the flow rate, and the temperature in the furnace, with certain ranges. Preliminary tests conducted on baseline NT154, Pack Cemented and HEEPS specimens, as well as several only reference samples, show the evidence of recession. The results from a recent 72 hour test (temp=1200°C, $\%H_2O$=47%, flow rate=18cm/s) are shown in Table I, ranked from best to worst.

Table I: Internal Recession Test Results

Samples	Normalized mass change (mg/cm2/hour) Run #3
Y2O3 Sample	-4.9E-04
Al2O3 Sample	-1.5E-03
Yttria stabilized Zirconia Sample	-2.6E-03
NT154 Pack Cementation Sample #12	-3.1E-03
NT154 Pack Cementation Sample #8	-3.3E-03
NT154 Pack Cementation Sample #13	-3.4E-03
Baseline NT154	-3.8E-03
NT154 HEEPS #1	-3.9E-03
NT154 Pack Cementation Sample #6	-4.4E-03
NT154 Pack Cementation Sample #11	-4.7E-03
NT154 HEEPS #2	-5.1E-03
Fused Quartz	-5.5E-03

2. NET SHAPE FORMING DEVELOPMENT (NSFD):

Under this task, the optimized green machining procedure (described in the previous quarterly report) was employed to fabricate four rotors of an Ingersoll-Rand design. One of the rotors has been densified (Figure 1), utilizing the new HIP process for improved as-processed (AP) surfaces. The dense rotor has an excellent average surface roughness (R_a) of 34 in. Several dimensions and blade profiles were measured on the dense rotor, using CMM. The dimensions are consistently on the low side with a maximum deviation of 0.012" from nominal. Upon further investigation, it has been determined that the new HIP process has a slightly different shrinkage than the old HIP process. The IR rotors were green machined according to the shrinkage seen with the old HIP process.

The rotor has been delivered to HT Lin at ORNL for mechanical testing. Biaxial disks from both the airfoils and hub region will be machined for mechanical property evaluation.

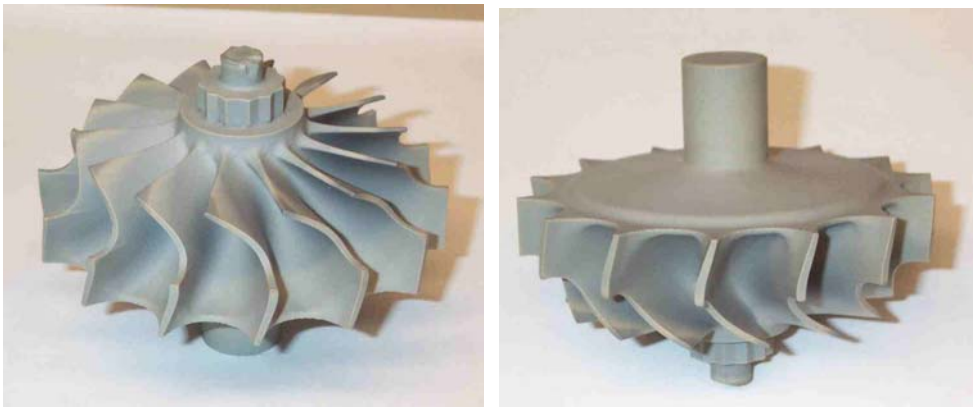

Figure 1: Dense NT154 Rotor of an Ingersoll-Rand Design

Status of Milestones

(1) Demonstrate a 40% improvement in the as-processed strength of Saint Gobain NT-154 silicon nitride (July 2004): ON SCHEDULE

Our baseline or starting average AP flexure strength for NT154 is 450-500 MPa, which we showed in Phase I and which is consistent with earlier ATTAP data. We are targeting a consistent improved AP strength of at least 650-700MPa, which would achieve the 40% DOE Milestone Goal.

We are encouraged that we can achieve the upper average 700 MPa goal and we have already achieved it on two occasions. We need to demonstrate it repeatable and are currently working to do so. We are in the process of demonstrating reliability and are currently making specimens for qualification at ORNL.

(2) Evaluate baseline recession resistance for uncoated and surface-modified NT154 (September 2004) and

(3) Develop a suitable surface modification procedure or EBC for test tiles and components to improve the recession resistance (December 2004): ON SCHEDULE

The development of an internal recession test will be instrumental in screening candidate solutions. The baseline NT154, as well as surface-modified NT154 from the initial experiments, has already been tested in the internal recession test. The results are shown above. Future samples will also be tested internally. Once a suitable sample has been produced, it will be forwarded to ORNL for Keiser Rig testing.

Industry Interactions

A visit to UTRC took place on March 15, 2004. Attendees included: Vimal K. Pujari, Oh-Hun Kwon, Ara Vartabedian, Bill Collins, Bob Licht and Bill Donahue. Discussions were held on our progress with the NT154 material and shape forming. Our most current material data base was provided to UTRC for rotor and vane life prediction calculations.

Problems Encountered

None

Publications/Presentations

"Reliable High Temperature Silicon Nitride and Components for Microturbine Applications", presented by Vimal K. Pujari at the 28th ACerS Cocoa Beach International Conference, January 29, 2004.

"Hot-Section Silicon Nitride Materials Development for Advanced Microturbines and Other Gas Turbine Component Applications", presented by Robert H. Licht at the 28th Annual Conference

on Composites, Materials and Structures, USACA ITAR Restricted Meeting, Cape Canaveral/Cocoa Beach, January 29, 2004.

Environmental Protection Systems for Ceramics in Microturbines and Industrial Gas Turbine Applications Part A: Conversion Coatings

S. D. Nunn and R. A. Lowden
Metals and Ceramics Division
Oak Ridge National Laboratory
P.O. Box 2008, Oak Ridge, TN 37831-6087
Phone: (865) 576-1668, E-mail: nunnsd@ornl.gov

Objective

Monolithic silicon nitride ceramics are currently the primary ceramic material being used in combustion engine environments and are under consideration as hot-section structural materials for microturbines as well as other advanced combustion systems. Under oxidizing conditions, silicon nitride will typically form a surface oxidation (silicate) layer. In a combustion environment, this silicate layer can undergo rapid degradation because of the corrosive and erosive effects of high temperature, high pressure, and the presence of water vapor. This degradation can severely limit the useful life of the ceramic in this environment. Thus, the development of an environmental protection system for the ceramic has become an essential goal for enabling the long-term utilization of these materials in advanced combustion engine applications.

One approach that is being pursued to produce an environmental protection system for silicon nitride is the formation of a surface conversion layer using the pack cementation process. Pack cementation has been used for many years to develop an oxidation protection coating on nickel-based superalloys that are used for hot-section components in gas turbine engines. A reactive gas atmosphere is used to change the composition and microstructure of the metal alloy at the surface of the component so that it will form a protective oxide film under normal operating conditions. The same approach can be used to form a modified surface region on silicon nitride ceramic components. By selecting an appropriate reactive atmosphere for the pack cementation process, the surface region can be modified to form ceramic compounds that may provide enhanced corrosion and erosion resistance in the combustion engine environment.

Highlights

Silicon nitride samples of Honeywell AS800, Kyocera SN281, and Saint Gobain NT154 were coated by pack cementation in air at 1400ºC. The coating packs contained the rare earth oxide Yb_2O_3, which had been identified in NASA and Kyocera studies as forming silicate compounds that are compatible with silicon nitride and stable in oxidizing environments. Silicon nitride samples that were coated in a powder pack of Yb_2O_3 alone formed surface layers containing mixtures of Yb_2SiO_5, $Yb2Si_2O_7$, SiO_2, and Yb_2O_3. When the powder pack consisted of Yb_2O_3 and Al_2O_3, the coated surfaces contained $YbAlO_3$, as well as $Yb_2Si_2O_7$ and some Al_2O_3 and mullite ($Al_6Si_2O_{13}$). These coated samples will be examined further for resistance to a moist, oxidizing environment.

Technical Progress

Initial tests were begun to evaluate the formation of ytterbium-containing coatings on silicon nitride substrates. Samples of Honeywell AS800, Kyocera SN281, and Saint Gobain NT154 silicon nitrides were heated in air to 1400ºC while embedded in powder packs containing Yb_2O_3. Two pack compositions were compared in the coating study: one contained only the rare earth oxide Yb_2O_3, the second consisted of a mixture of Yb_2O_3 and Al_2O_3. The processing variations and the coating phases that were formed are summarized in Table 1.

Table 1. Processing variations and coating phases identified by XRD.

Silicon Nitride Substrate	Pack Composition	X-ray Diffraction Phase Analysis
AS800	Yb_2O_3	Yb_2O_3, Yb_2SiO_5, $Yb_2Si_2O_7$
AS800	$Yb_2O_3 – Al_2O_3$	Al_2O_3, $Yb_2Si_2O_7$, Mullite, $YbAlO_3$
NT154	Yb_2O_3	Yb_2O_3, SiO_2, $Yb_2Si_2O_7$
NT154	$Yb_2O_3 – Al_2O_3$	$Yb_2Si_2O_7$, Al_2O_3, $YbAlO_3$, Mullite
SN281	Yb_2O_3	Yb_2O_3, $Yb_2Si_2O_7$, Yb_2SiO_5
SN281	$Yb_2O_3 – Al_2O_3$	$Yb_2Si_2O_7$, Al_2O_3, $YbAlO_3$, Mullite

The silicon nitride samples that were coated in a powder pack of Yb_2O_3 alone formed surface layers containing mixtures of Yb_2O_3, Yb_2SiO_5, and/or $Yb2Si_2O_7$. Some SiO_2 was observed in the NT154 sample coating. The ytterbium silicates have been identified in NASA and Kyocera studies as being compatible with the thermal expansion coefficient of silicon nitride and stable in oxidizing environments. When the powder pack consisted of Yb_2O_3 and Al_2O_3, the coated surfaces contained the aluminate compound $YbAlO_3$, as well as $Yb_2Si_2O_7$. There was also some Al_2O_3 and mullite ($Al_6Si_2O_{13}$) identified in these coatings. Additional variations of the coating process using Yb_2O_3 are planned to better refine and control the coating phases that are formed. The coatings will be examined further for resistance to the oxidizing and corrosive conditions of the high-temperature gas turbine engine environment.

A simple testing system is being prepared to allow evaluation of coated samples at elevated temperature in a high-moisture-content atmosphere. The setup will be similar in function to the rig being used by researchers at NASA. A laboratory steam generator has been ordered to be used with a tube furnace to provide an environment that simulates the gas turbine engine. Although the turbine engine pressure will not be simulated, the temperature and water vapor levels should provide a good screening mechanism for examining the durability and protective characteristics of the coatings produced on the various silicon nitride substrates.

Status of Milestones

Evaluate the corrosion resistance of strontium aluminate-type and ytterbium-containing surface conversion coatings on silicon nitride in a simulated combustion atmosphere. (Sept. 2004)

Industry Interactions

Obtained a sample of composite material from GE Aircraft Engines for evaluation of applying a protective coating by pack cementation.

Met with Kennametal to discuss status of SiAlON production and possible protective coating compounds.

Problems Encountered

None

Publications and Presentations

None

Polymer Derived EBC for Monolithic Silicon Nitride

Rishi Raj and Sudhir Brahmandam
University of Colorado
Boulder, Co
Phone: (303)492-1029, E-mail: Rishi.Raj@Colorado.EDU

Objective

The overall objective of this work is to develop novel EBCs for monolithic silicon nitride turbine blades from oxide/non-oxide based precursor derived ceramics, for example, ZrO_2-SiCN. The statement of work includes three tasks:

A. Thermodynamic and kinetic stability of oxides with SiCN in the temperature range of 1473 to 1673 K will be evaluated.
B. Oxidation kinetics of oxide-SiCN structures will be studied to discern if the interfacial bonding will avert formation of silica.
C. Structures prepared in 'B' will be tested in the Keiser Rig at ORNL.

Highlights

•Composites with SiCN content from 2 to 50 vol%, corresponding to SiCN interface thicknesses from 1 μm to 20 nm, have been prepared. These samples are being used to study the oxidation behavior by microstructural analysis (coating thickness and reactions at zirconia-SiCN interfaces. A second type of specimen geometry has been developed to study the oxidation behavior both microstructurally and by weight change. This geometry is in the form of fibers, which can be easily sectioned for microstructural information, and because of high surface to volume ratio can be studied by change in weight.

•Hydrothermal corrosion setup have been fabricated to study the oxidation and corrosion behavior of the composites in air and water vapor for temperatures up to 1673 K, at flow rates of up to 100 cm s^{-1}.

Technical Progress (Cumulative)

Review of the literature shows that dense SiCN samples could only be made when at least one dimension of the sample is < 500 μm. Further, there is no reported data on the processing of bulk SiCN based composites. Therefore, initial studies were aimed at developing a processing route to obtain dense zirconia – SiCN. These studies revealed that the presence of zirconia particles in the SiCN matrix can be hot-pressed to full density. The following samples have been made.

Samples made from Oxide Powders

Earlier work has focused on processing particulate composites made from SiCN and zirconia, and alumina. These composites are called Type I if SiCN phase is continuous and Type II if the SiCN phase is in particulate form. Table 1 lists the samples prepared and sent for Keiser Rig evaluation in Dec. 2003.

Table 1: Samples sent for Keiser Rig evaluation.

Sample	Composition	Oxide Particle Size (μm)	Microstructure Type$_2$	Preparation Method*	Comments
S1	ZrO_2-8v%SiCN	0.5	I	A	Nearly dense
S2	ZrO_2-15v%SiCN	0.5	II	B	Nearly dense
S3	ZrO_2-8v%Al_2O_3	0.5	I	A	Porous
S4	ZrO_2-15v%Al_2O_3	0.5	II	B	Porous

**Process A*: Mixing oxide powders in Ceraset. Cross-linking at 673 K. Warm pressing at 673 K and hot pressing at 1573 K. *Process B*: Mixing oxide and SiCN in powder form. Hot pressing at 1573 K.

Subsequent studies have shown that a modification of 'process A' gives nearly dense oxide-SiCN composites with Type I microstructures even with SiCN content as high as 50 vol%. Details for this process are given in the previous quarterly report. The BET surface area analysis indicated that the nano-porosity in these samples can range from 0.5 m^2/g to 4 m^2/g. We are pressing ahead to obtain as low porosity in our samples, reproducibly. Figure 1 shows the XRD data for these composites. The peaks correspond to cubic zirconia, indicating that the processing route did not cause an appreciable reaction between SiCN and zirconia.

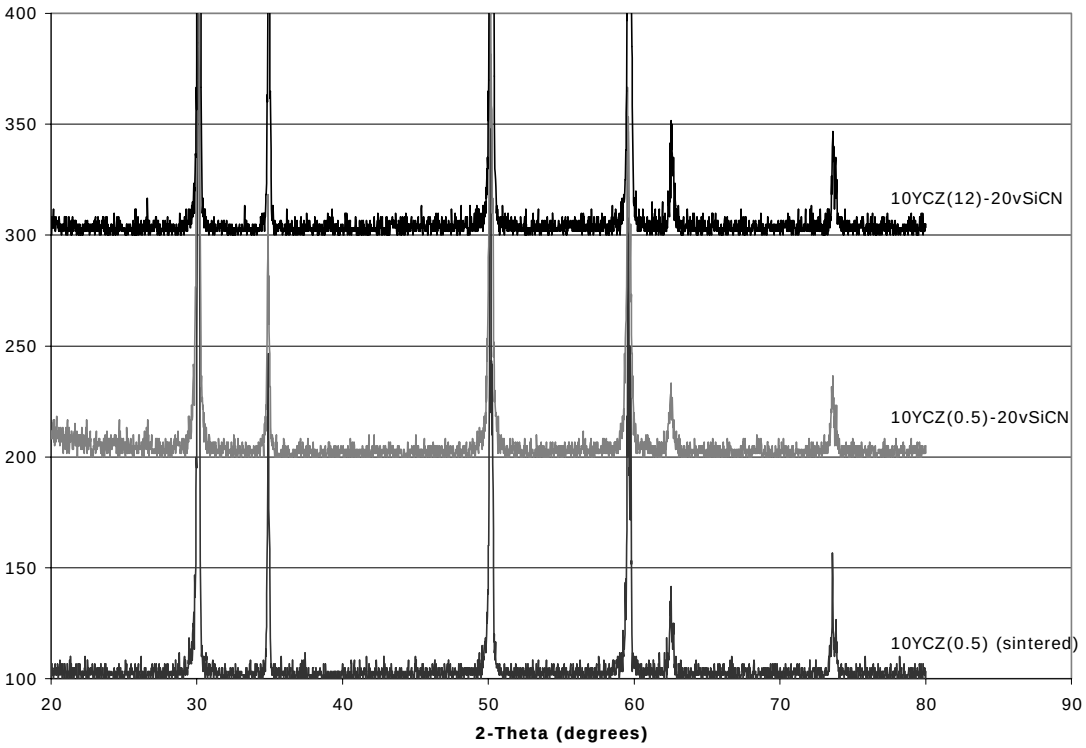

Figure 1: XRD data of zirconia – 20v%SiCN composites. Cubic zirconia data shown for comparison.

<u>High Surface area Samples</u> made from Polymer Precursors of Zirconia

Samples described under (1.) above are suitable for the study of oxidation by microstructural analysis, that is, by the study of the oxidation layer on the surface of the specimen and the reactions at SiCN-ZrO2 interfaces deep within the sample. These studies of oxidation behavior have begun.

A second method of studying oxidation is to measure the change in weight of the sample with oxidation. For this purpose high surface area samples are needed. In this task we are preparing these samples directly from the polymer route using organic precursors for both the oxide and the silicon carbonitride. The weight change results must be combined with microstructural analysis. The shape of a fiber enables both types of studies to be done easily. The microstructural evaluation can be done by sectioning the fiber, and the weight change study is possible because the fibers have a high surface to volume ratio. Fiber samples with 10-20 vol% ZrO_2 are now being prepared by adding Zr-n-propoxide to ceraset. These fibers have a diameter of 5-10 μm.

Design and Construction of a Set Up for First-Phase Oxidation Studies

In this study we are evaluating new materials. Different microstructures and sample geometries are being considered to understand the oxidation behavior of zirconia-silicon carbonitride materials. Therefore, there is a need to have a set-up that can provide first-phase information on the oxidation behavior of this new materials in humid environments before the samples are sent in for evaluation in the Keiser Rig. A setup has been fabricated to study the hydrothermal corrosion behavior in highly humid conditions with vapor flow rates of up to 100 $cm.s^{-1}$ and temperatures up to 1673 K. Figure 2 gives a schematic illustration of this unit.

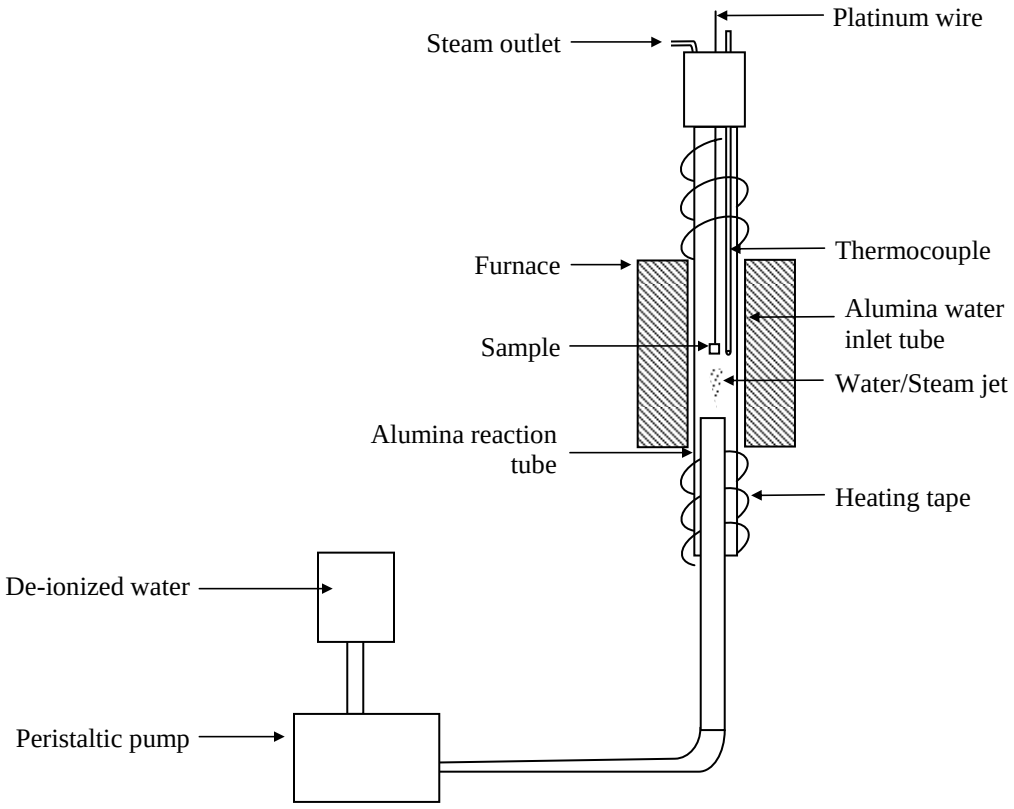

Figure 2: Hydrothermal corrosion testing unit

The hydrothermal setup consists of injecting a jet of water at a controlled flow rate into an alumina reaction tube that is heated to the testing temperature in a high temperature tube furnace. The exposed portions of the reaction tube are heated to > 400 K using heating tapes to prevent condensation of water inside the tube. The sample is suspended in the hot zone of the reaction tube using a platinum wire.

Status of Milestones

The following experiments are planned for the coming quarter:

Task A: Interfacial reactions in SiCN-ZrO_2 composites as a result of oxidation in humid environments.

Status: Good samples of the composites with Type I and Type II microstructures have now been prepared. They will be tested during this period. The hydrothermal oxidation unit will be calibrated with silicon nitride samples during the next quarter.

Task B: Phase stability of SiCN-ZrO_2 microstructures.

Status: Power samples for x-ray studies have been prepared and will be characterized next quarter.

Task C: Testing in the Keiser Rig

Status: Preliminary samples were sent to Karren More in December 2003. However, these samples were not dense and they may have cracked upon heating to the oxidation temperature. We are now preparing good samples, and studying them in Boulder to see if they are indeed promising. They will then be sent to ORNL in July 2004, so that the results from the Keiser testing can be reported in the EBC workshop in mid November.

Industry Interactions

There are on-going interactions with Honeywell, Inc. This work is presently concentrated on the development of processes to make multilayer coatings from SiCN and ZrO_2. After preliminary experiments at Boulder the coatings will be sent to Honeywell for evaluation.

Problems Encountered

Preparation of dense SiCN-ZrO2 samples has taken considerable development. Now, specimens with low porosity (0.5 m^2/g) are being prepared. This has caused some delay in meeting the milestones. However, this delay would be overcome in the coming quarter.

Publications and Presentations

None

Environmental Protection Systems for Ceramics in Microturbines and Industrial Gas Turbine Applications: Slurry Coatings

B. L. Armstrong, K. M. Cooley, and G. H. Kirby
Metals and Ceramics Division
Oak Ridge National Laboratory
P. O. Box 2008, Oak Ridge, Tennessee 37831-6063
Phone: (865) 241-5862, E-mail: armstrongbl@ornl.gov

Objectives

Silicon-based monolithic ceramics are candidate hot-section structural materials for microturbines and other combustion systems. The performance of silica-forming ceramic materials in combustion environments is, however, severely limited by rapid environmental attack caused by the combination of high temperature, high pressure, and the presence of water vapor. Thus, the development of environmental protection systems has become essential for enabling the long-term utilization of these materials in advanced combustion applications.

Similar to thermal barrier coatings for nickel-based super alloys that utilize a specialized oxide surface layer and a metallic bond coat, successful environmental protection systems for ceramics and ceramic composites will likely utilize multiple layers and complex combinations of materials. Most recent efforts have focused on the selection and deposition of the oxide surface layer, and due to numerous factors, the majority of the candidates have been from the aluminosilicate family of oxide ceramics. Stable rare-earth silicate deposits have been found on component surfaces after recent engine and rig tests, indicating there may be other stable oxide compositions that have not been fully investigated. Thin coatings of selected silicate compositions will be deposited on test coupons using a variety of techniques. The specimens will then be exposed to simulated high-pressure combustion environments and materials that demonstrate good potential will be investigated further

Highlights

Mullite coatings were formed by dipping SiC, Si_3N_4, and silicon substrates into concentrated, mullite suspensions of tailored rheological behavior. Dried coatings were crack-free and fully densified at 1350^{o}C, which is considerably below the temperature requirement for densification of mullite in bulk form (1600^{o}C).

Technical Progress

Optimization of Mullite-PEI Suspension Rheology

Work continued on the optimization of mullite (MULCR®, Baikowski International Corporation, Charlotte, NC) slurry rheology for a dip coating process. Mullite was used as a surrogate material for the yttrium disilicates in order to optimize general rheology and dip

conditions. A cationic polyelectrolyte (polyethylenimine or PEI, Polysciences, Warrington, PA), with a weight average molecular weight (M_w) of 10,000 g/mole and one amine group (NH) per monomer unit was implemented as a rheological modifier for this system. Concentrated mullite suspensions (45 vol% solids) were prepared at a constant pH of 7 and varying PEI concentration. The suspensions were ultrasonically treated for 5 min to break up weak agglomerates and mixed on a shaker table for 24 h to obtain equilibrium behavior. Rheological measurements were carried out using a controlled stress rheometer (Rheometric Scientific SR5, TA Instruments, New Castle, DE) in stress viscometry and oscillatory stress modes to measure the apparent viscosity and elastic modulus, respectively.

The apparent viscosity is plotted as a function of applied shear stress in Fig. 1 for suspensions of varying PEI concentration. The degree of shear-thinning decreased with increasing PEI concentration until nearly Newtonian flow behavior was obtained at a PEI concentration of 0.2 mg/m^2 mullite. These suspensions exhibited stable flow behavior over a 15 day time span, as shown by the data in Fig. 2. The elastic modulus is plotted as a function of applied shear stress in Fig. 3 for suspensions of varying PEI concentration. Solid-like behavior, indicative of colloidal gels, was observed for suspensions with PEI concentrations less than 0.2 mg/m^2 mullite. The linear elastic modulus and yield stress decreased with increasing PEI concentration until a transition from gel- to fluid-like behavior occurred at 0.2 mg/m^2 mullite.

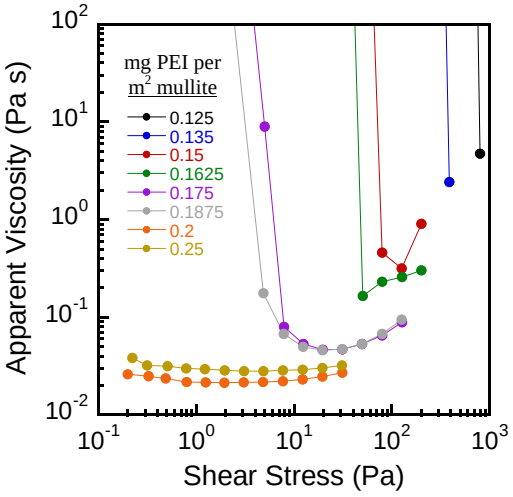

Fig. 1. Apparent viscosity as a function of shear stress for concentrated mullite suspensions (45 vol% solids) of varying PEI concentration. Note, the solid lines merely guide the eye.

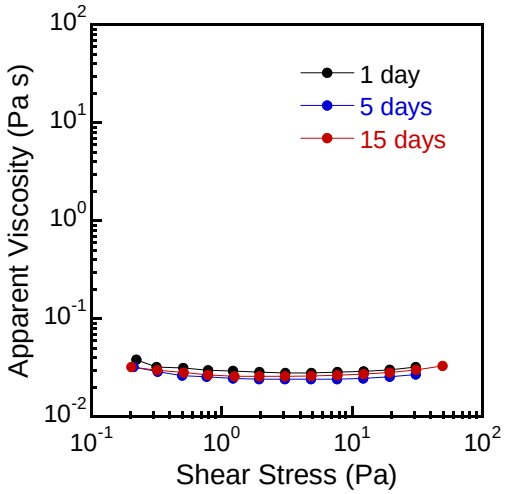

Fig. 2. Apparent viscosity as a function of shear stress for concentrated mullite suspensions (45 vol% solids, 25 mg PEI/m^2 mullite) aged for varying times.

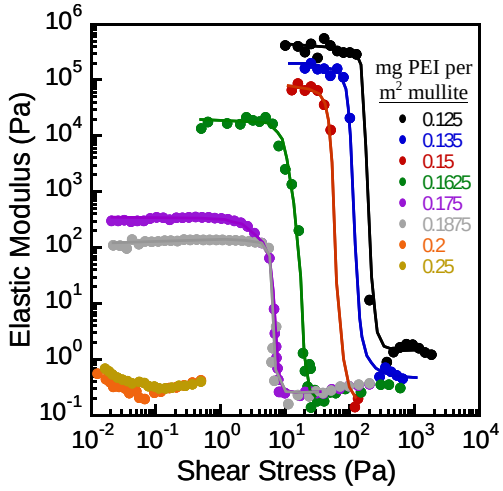

Fig. 3. Elastic modulus as a function of shear stress for concentrated mullite suspensions (45 vol% solids) of varying PEI concentration. Note, the solid lines merely guide the eye.

Slurry Coatings

Substrates of varying composition, including silicon carbide (Hexaloy, Carborundum Co., Niagara Falls, NY), silicon nitride (AS800, Honeywell Ceramic Components, Torrance, California), and metallic silicon, were dipped into concentrated mullite suspensions (45 vol%) of varying PEI concentration. The substrates were dipped at rate of 85.7 mm/min, submerged for 1 min, and withdrawn at a rate of 85.7 mm/min. Coated substrates were dried under ambient conditions and are displayed in the image gallery in Fig. 4. Excellent coatings were obtained from mullite suspensions with 0.1625 - 0.175 mg PEI/m^2 mullite surface. Mullite suspensions with less than 0.1625 mg PEI/m^2 mullite resulted in thick, uneven coatings. The quality of the coatings decreased with decreasing PEI concentration. These features result from a particle gel network that is too strong, i.e., when the linear elastic modulus is greater than ~ 10 kPa. Mullite suspensions with 0.1875 mg PEI/m^2 mullite or greater resulted in coatings with three types of defects: drying defects or "dimples", pores due to entrained air bubbles, and thickness gradients. All of these defects stem from a particle gel network that is too weak, i.e., when the linear elastic modulus is less than ~ 100 Pa. For example, drying defects arise from solvent wicking and particle migration from the center of each coated face to drying fronts that initiate, and converge inward from the corners and edges.[1] Pores arise from air bubbles that are entrained in the low viscosity suspensions and quickly migrate to the suspension/substrate interface during dipping. Thickness gradients result from dripping and beading of the suspensions at the bottom of the substrate surface.

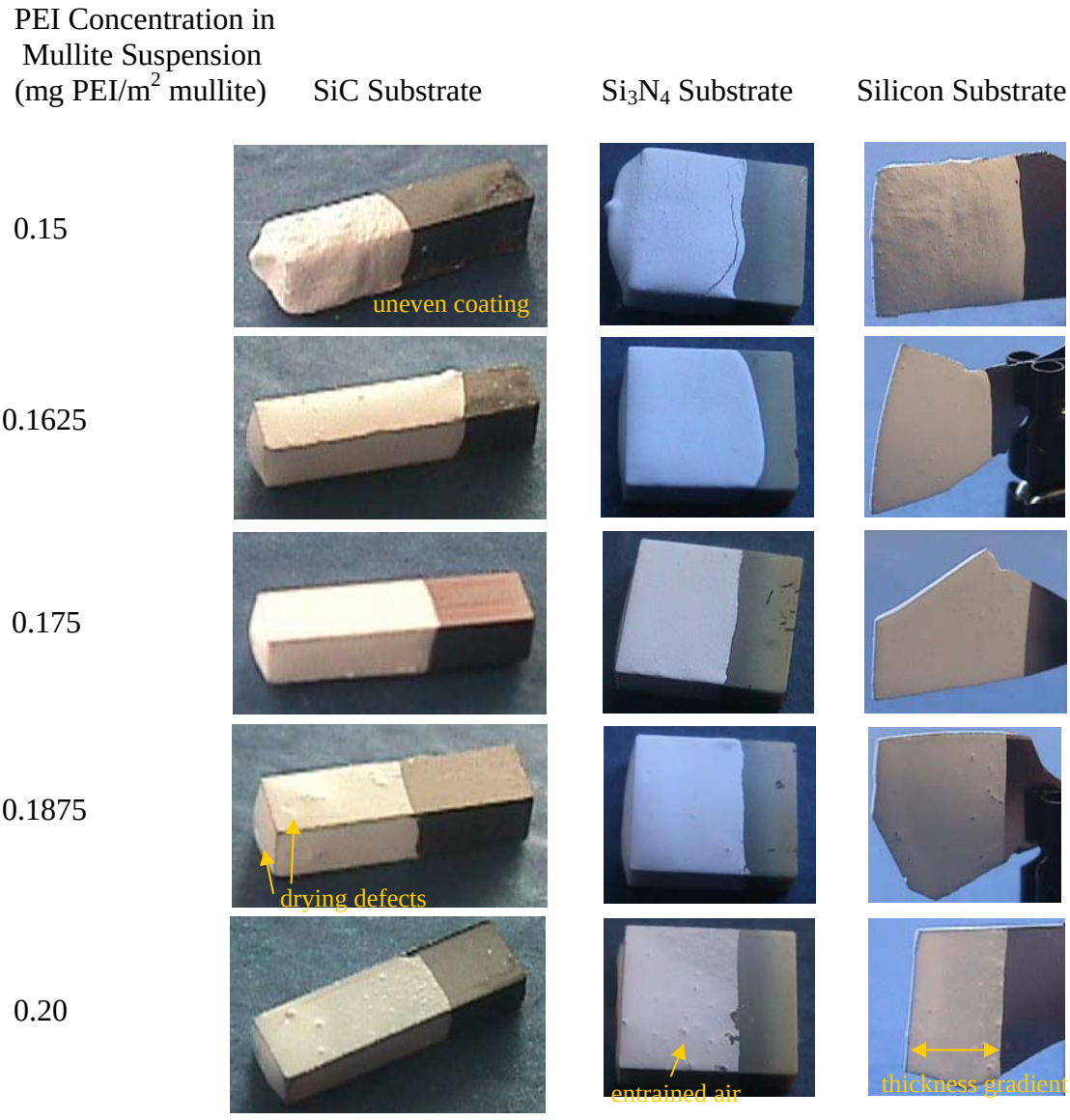

Sintering Behavior

Early results suggest that the sintering atmosphere plays an important role in obtaining adherent, dense coatings. Adherent coatings have been obtained in an oxygen atmosphere, but not in argon or nitrogen. It is believed that a thin, silica rich reaction layer may form to provide a bond coat in oxygen, but not in argon or nitrogen. Furthermore, the coatings likely react with nitrogen to form AlN, leading to a net volume expansion and spallation of the coating. Preliminary results show that dense coatings are achieved at 1350^{o}C, which is significantly lower than the temperature requirement for densification of mullite in bulk form (1600^{o}C). These results demonstrate the feasibility of dip coating and sintering environmental barrier coatings onto functional components. The effect of sintering temperature and atmosphere on coating properties after exposure to high temperature steam are in-process.

Development of a Sacrificial Coating

No work to report this quarter.

Status of Milestones

Evaluate the protective capacity yttrium disilicate deposited by a slurry-based process on silicon nitride in a simulated combustion environment. (September 2004)

Industry Interactions

Discussions with UTRC and GE have continued. This project has also collaborated with an ARTD Fossil Energy project on Corrosion Resistant Coatings.

Problems Encountered

None

Publications

None

References

1. C. J. Martinez, J. A. Lewis, "Rheological, Structural, and Stress Evolution of Aqueous Al_2O_3:Latex Tape-Cast Layers," *J. Am. Ceram. Soc.*, **85** [10] 2409-16 (2002).

Failure Mechanisms in Coatings

J. P. Singh, K. Sharma, and P. S. Shankar
Energy Technology Division
Argonne National Laboratory
Argonne, IL 60439
Phone: (630) 252-5123, E-mail: jpsingh@anl.gov

Objective

The purpose of this proposed research is to identify failure mode(s), understand and evaluate failure mechanisms, and develop appropriate test methods and protocols to characterize the integrity and predict failure of environmental and thermal barrier coatings for advanced turbine applications.

Technical Highlights

Four-point flexure strength of AS800 silicon nitride (Si_3N_4) specimens coated with different compositions of tantalum oxide (Ta_2O_5) based environmental barrier coating (EBC) has been evaluated. The measured strength of AS800 specimens coated with Ta_2O_5 + 3wt.% Al_2O_3 + 3wt.% La_2O_3-EBC (543±6 MPa) was higher than that of the specimens coated with Ta_2O_5 (458±20 MPa) or Ta_2O_5 + 3wt.% Al_2O_3-EBC (351±2 MPa). On the other hand the strength of these coated specimens was lower than that of the uncoated specimens (709±58 MPa). Fractographic analysis indicated that failure occurs at the EBC/substrate interface, which is associated with pores/voids, and microstructural discontinuities.

Technical Progress

Effort this quarter concentrated on evaluating the four-point flexure strength of AS800 Si_3N_4 specimens coated with different compositions of Ta_2O_5-EBC. AS800 substrates (50 mm x 26 mm x 4 mm) coated with Ta_2O_5 + 3wt.% Al_2O_3, and Ta_2O_5 + 3wt.% Al_2O_3 + 3wt.% La_2O_3 EBCs were received from Northwestern University/Honeywell. The EBCs had been deposited using small particle plasma spray process [1] on the substrates, which had been preheated to 450°C following a 1250°C soak. Four-point flexure bar specimens of dimension 26 mm x 2 mm x 1.5 mm were machined from the coated substrates using diamond saw. Four bars for each composition were tested according to the ASTM C1161-94 specification (Configuration A) with the coating side loaded in tension.

Figure 1 shows the measured four-point flexure strength of AS800 specimens coated with different compositions of the Ta_2O_5 based EBCs. For comparison, the measured strength of uncoated AS800 specimens (Quarterly Report July-September 2003) is also shown in the figure. The strength evaluation of the coated specimens was based on the analysis of a composite beam in bending. For the strength calculations, elastic modulus of EBC was taken as 90 GPa for all the EBC compositions. It can be clearly seen from Figure 1 that the flexure strength (543±6 MPa) of AS800 coated with Ta_2O_5 + 3wt.% Al_2O_3 + 3wt.% La_2O_3 EBC is the highest among the three EBC compositions. However, all the three sets of EBC-coated AS800 specimens have a

lower strength than the uncoated AS800 specimens. The observed decrease in strength for the EBC-coated AS800 specimens may be related to the presence of residual stresses at the interface arising from thermal expansion mismatch between the AS800 substrate and the EBC.

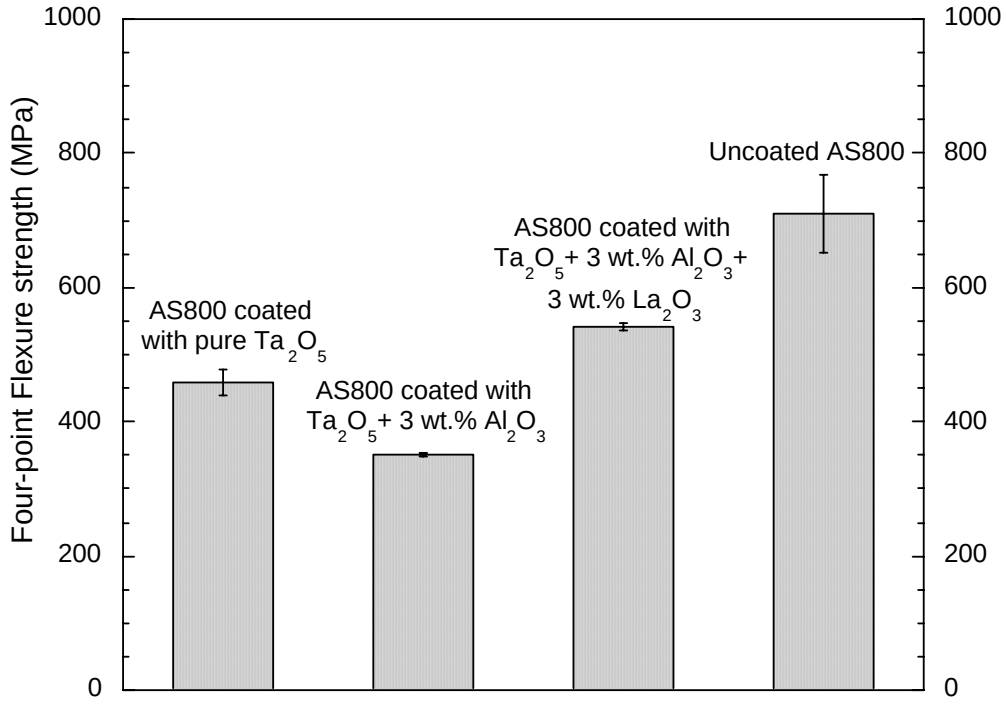

Figure 1. Four-point flexure strength of AS800 Si_3N_4 specimens coated with different compositions of Ta_2O_5 based EBC. The flexure strength of uncoated AS800 is also shown.

Fractographic evaluation of failed four-point flexure bars was performed to identify failure origin and characterize critical flaws. Figure 2 shows the fracture surface and a critical flaw (voids/pores) in an AS800 flexure bar specimen coated with Ta_2O_5 + 3wt.% Al_2O_3 + 3wt.% La_2O_3-EBC. Similar fracture morphology and critical flaws were observed in all the specimens of this composition. As shown in Figure 3, failure in EBC specimens with Ta_2O_5 + 3wt.% Al_2O_3 composition primarily initiated at the EBC/substrate interface, apparently from microstructural discontinuities. Currently, effort is in progress to understand the effect of compositional variations in Ta_2O_5 based EBCs on the flexural response of EBC-coated AS800 Si_3N_4 specimens. Furthermore, microindentation testing and stress analysis at the EBC/substrate interface are in progress to understand the observed strength degradation of the coated AS800 specimens as compared with the uncoated specimens.

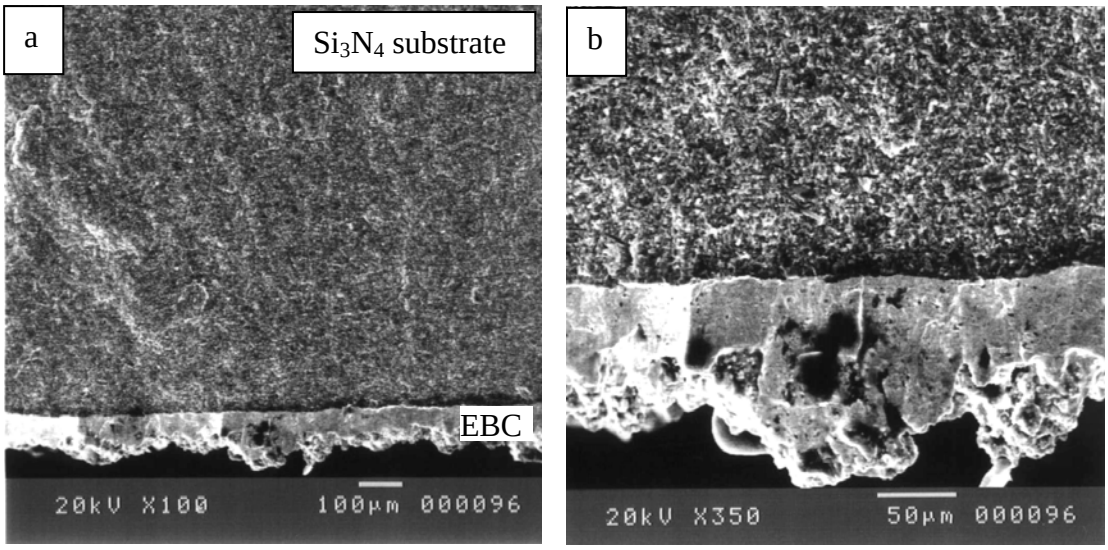

Figure 2. Fracture surface of AS800 coated with Ta_2O_5 + 3wt.% Al_2O_3 + 3wt.% La_2O_3. (a) Fracture markings at the failure origin, and (b) higher magnification image showing critical flaw (voids/pores) at the failure/origin.

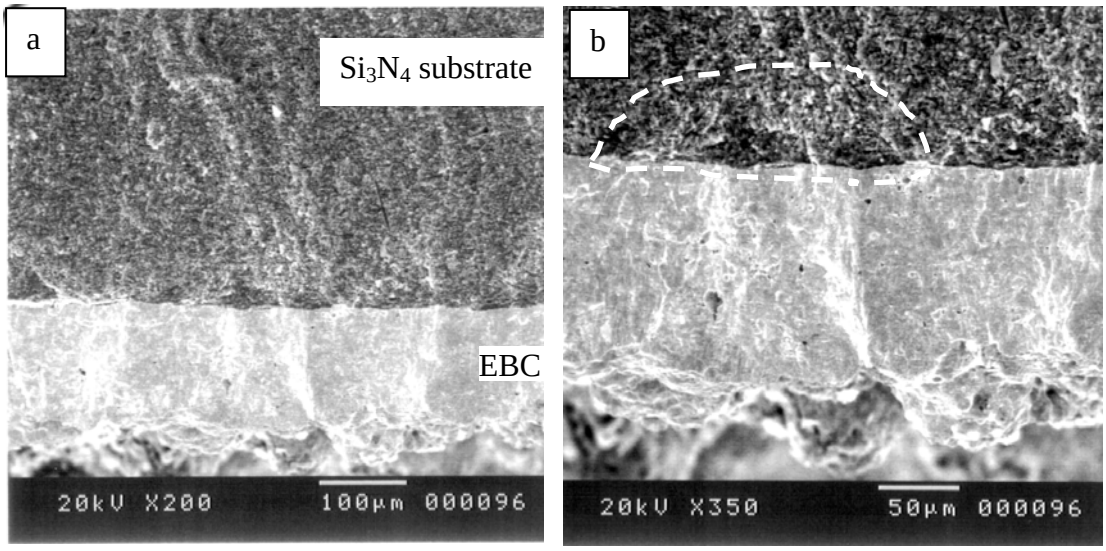

Figure 3. Fracture surface of AS800 coated with Ta_2O_5 + 3wt.% Al_2O_3, showing the (a) fracture markings, and (b) location of failure initiation at the EBC/substrate interface.

Status of Milestones

Complete evaluation of the effects of compositional variation in Ta_2O_5-based EBCs on mechanical behavior of coated Si_3N_4 (AS800) substrates that are being developed at Northwestern University/Honeywell. September 2004. On Schedule.

Industry Interactions

Discussion on the results of mechanical and microstructural evaluation of Ta_2O_5-coated AS800 Si_3N_4 specimens was continued with Northwestern University/Honeywell.

Problems Encountered

None

Publications/Presentations

K. Sharma, P. S. Shankar, and J. P. Singh, "Mechanical and Fractographic Evaluations of Si_3N_4 substrates with Environmental Barrier Coatings," presented at the 106th American Ceramic Society Annual Meeting and Exposition, Indianapolis, IN, Apr 18-21, 2004.

Reference

1. M. Moldovan, C. M. Weyant, D. L. Johnson, and K. T. Faber, "Tantalum Oxide Coatings as Candidate Environmental Barriers," J. Thermal Spray Technology 13 (1) 51-56 (2004).

High-Temperature Diffusion Barriers for Ni-Base Superalloys

B. A. Pint, K. M. Cooley and J. A. Haynes
Metals and Ceramics Division
Oak Ridge National Laboratory
Oak Ridge, TN 37831-6156
Phone: (865) 576-2897, E-mail: pintba@ornl.gov

Objective

Nickel-base superalloys require coatings to improve their high temperature oxidation resistance, particularly when a thermal barrier coating is employed. The underlying oxidation-resistant metallic coating or bond coat is degraded by the loss of Al due to oxidation, but much more Al is lost due to interdiffusion with the superalloy. Loss of Al causes diffusion aluminide coatings to undergo phase transformations, which likely cause deformation of the bond coat surface and subsequent loss of the protective alumina scale and the overlying thermal protection layer. The goal of this program is to fabricate and assess potential compounds for use as high-temperature diffusion barriers between coating and substrate. Ideally, the barrier would act to reduce the inward diffusion of Al, as well as the outward diffusion of substrate elements (such as Cr, Re, Ta, W), which generally degrade the oxidation resistance of the coating. The work is motivated by previous experimental results which suggested some compositions that exhibited diffusion-barrier capabilities. A secondary objective is to demonstrate routes to fabricating diffusion aluminide coatings incorporating a diffusion barrier using chemical vapor deposition (CVD).

Highlights

Electron microprobe analysis of Pt-Hf coatings revealed that although a layer with composition similar to the target phase of $HfPt_3$ (Engel-Brewer compound) formed during heat-treatment of Pt-Hf thin films below 1000°C, this phase was not stable. The $HfPt_3$-like phase either completely dissolved during short-term CVD aluminizing at 1100°C or else began to be diluted by the interdiffusion processes. Subsequent experiments heat treated Pt-Hf thin films at temperatures higher than 1000°C, the temperature at which a rapid exothermic reaction between Pt-Hf is reported to occur. Again, the Pt-Hf rich phase was observed to be unstable after CVD aluminizing at 1100°C.

Technical Progress

Electron Microprobe Analysis of Pt-Hf Coatings

The deposition of Pt and Hf layers on low sulfur René N5 substrates was described in prior reports. Specimens with Pt-Hf thin films were characterized by electron microprobe analysis (EPMA) for determination of the composition of the coatings after heat-treatment and after aluminizing. Specimens were heat treated for 1h at 500°C in order to relieve stress in the sputtered thin films, and then at higher temperatures to promote interdiffusion between the deposited Hf and Pt layers and the substrate. The temperature 900°C was initially selected since it is below the temperature at which a rapid exothermic reaction is reported to occur between Pt and Hf (1000°C). However, subsequent work looked at higher temperatures. The heat treated coatings were then aluminized. In order to compare specimens as accurately as possible, each specimen disc was first heat treated and then 30% of the specimen was cut off with a diamond saw and mounted for metallographic preparation. The remaining specimen was then aluminized via a low activity CVD process described in previous reports.

Two sets of samples were examined with a 900°C heat treatment for 2h: PHA5 has 3μm of Pt and

1µm of Hf and PHB5 has 5µm of Pt and 1µm of Hf. Figure 1 shows the cross-section and composition profile of PHA5 after both heat treatments but before aluminizing. A three-layer structure was present above the superalloy. The porous, outer layer of the coating was about 3 µm thick. It was Pt-rich but contained significant amounts of Ni and smaller amounts of Al, Hf, Co and Cr. The center layer was mostly dense, with a composition 69.5 Pt-20.9Hf-6.2 Ni-1.6 Al (at%) at approximately 4 µm below the surface. This layer had a composition similar to $HfPt_3$, although Pt-rich. The EPMA profile shows a minimum in both the Al and Ni contents within this phase. This result suggests a low solubility of Al and Ni in the Hf-Pt phase, which would be a positive characteristic for a diffusion barrier. The innermost layer of the coating was rich in Ni, Pt and Al.

Figure 2 shows similar results for the specimen after CVD aluminizing for 1h at 1100°C. Again three layers are visible. The outer layer is the typical dense, β-NiAl expected after CVD aluminizing. The outer surface of this layer had very high Al (47.2 at%) and Ni (40.4 at%) contents, with a significant amount of Pt (8.3 at%) present. The composition of the thin central layer showed a minimum in Al and Ni content, but there was only a slight peak in Pt and Hf. This central layer appears to be the remnant of the $HfPt_3$ layer after significant dissolution. The thicker innermost layer is the typical interdiffusion zone present in a CVD aluminide coating.

The second set of samples had a thicker initial Pt layer. Figure 3 shows the composition and cross-section after heat treatment of PHB5. A similar three-layer coating was observed in this case. Figure 3a shows that there was a Pt-Hf peak at approximately 4µm, similar to Figure 1a. The composition was similar to $HfPt_3$, but was again Pt rich. The surface composition of the outer layer was approximately 70 at% Pt, 19 at% Ni, 4 at% Al, 2.6 at% Co. The most obvious microstructural difference in Figs. 1b and 3b is the thinner interior layer in the latter case. The reason for this difference is not apparent. There do appear to be more voids in Figure 3b. These may have inhibited interdiffusion. Also, the thicker Pt layer may have had a higher residual stress, which could degrade adhesion with the inner Hf layer.

Figure 4 shows the cross-section and composition profile for PHB5 after aluminizing for 1h at 1100°C. The higher Pt content had a significant effect on the aluminized composition. The Pt-Hf

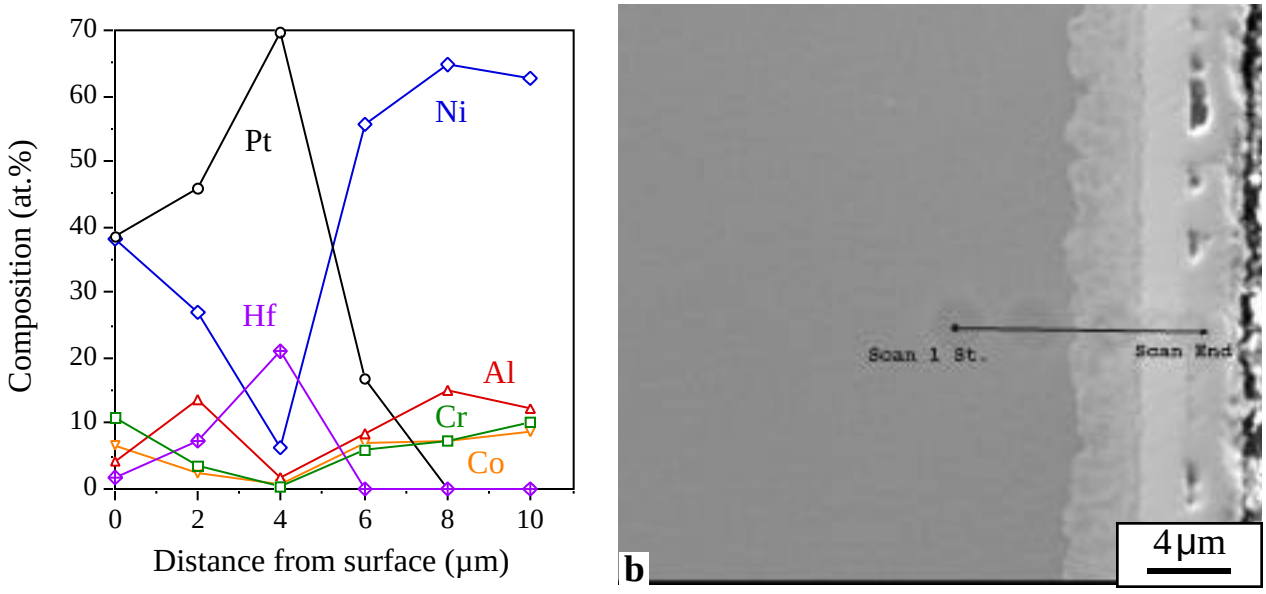

Figure 1. (a) EPMA profile of PHA5 after heat treatment. (b) micrograph of region analyzed.

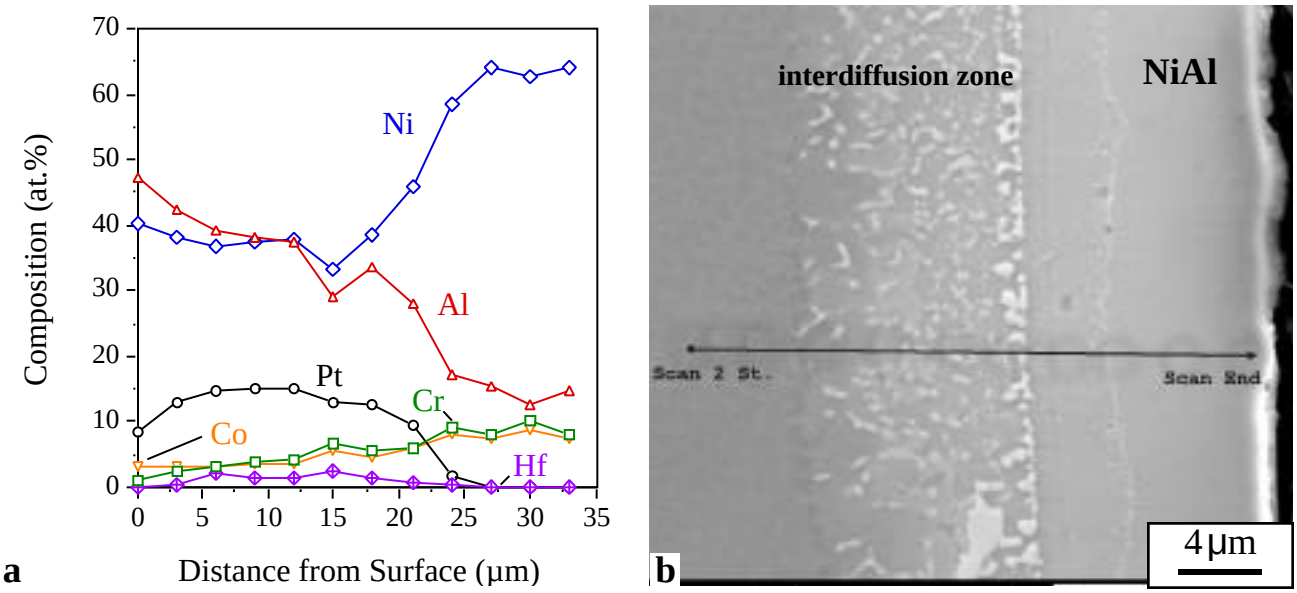

Figure 2. (a) EPMA profile of PHA5 after heat treatment and aluminizing. (b) micrograph of region analyzed.

layer is more evident in this case and the Al content of the coating is much lower. However, the Al content at the surface is very high (55%). The Hf content in the outer layer is much higher than in the other aluminized coating, suggesting that there may have been a slightly thicker Hf layer in this case. While these results are promising, it is worth noting that dilution of the Hf-Pt layer has already begun to occur on a limited basis after 1h of aluminization and will likely continue for longer aluminizing times.

Heat treatments above 1000°C

Since the 900°C heat treatment did not result in a stable $HfPt_3$ phase, a higher temperature anneal was tried. An exothermic reaction between Hf-Pt was reported in the literature above 1000°C and there

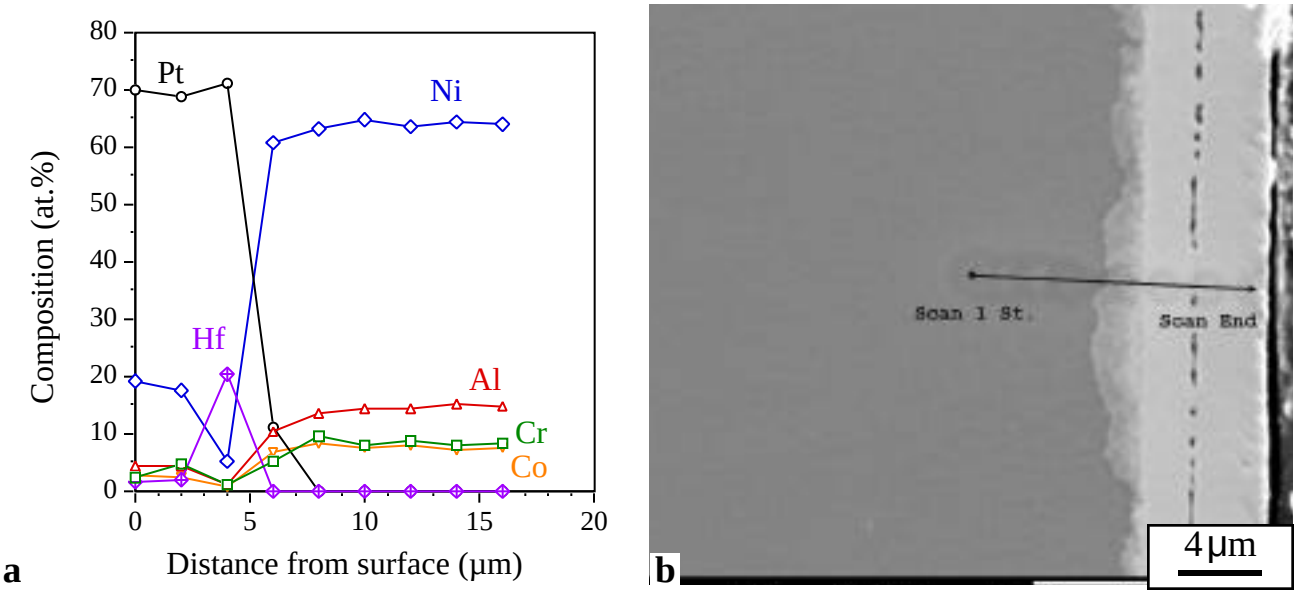

Figure 3. (a) EPMA profile of PHB5 after heat treatment. (b) micrograph of region analyzed.

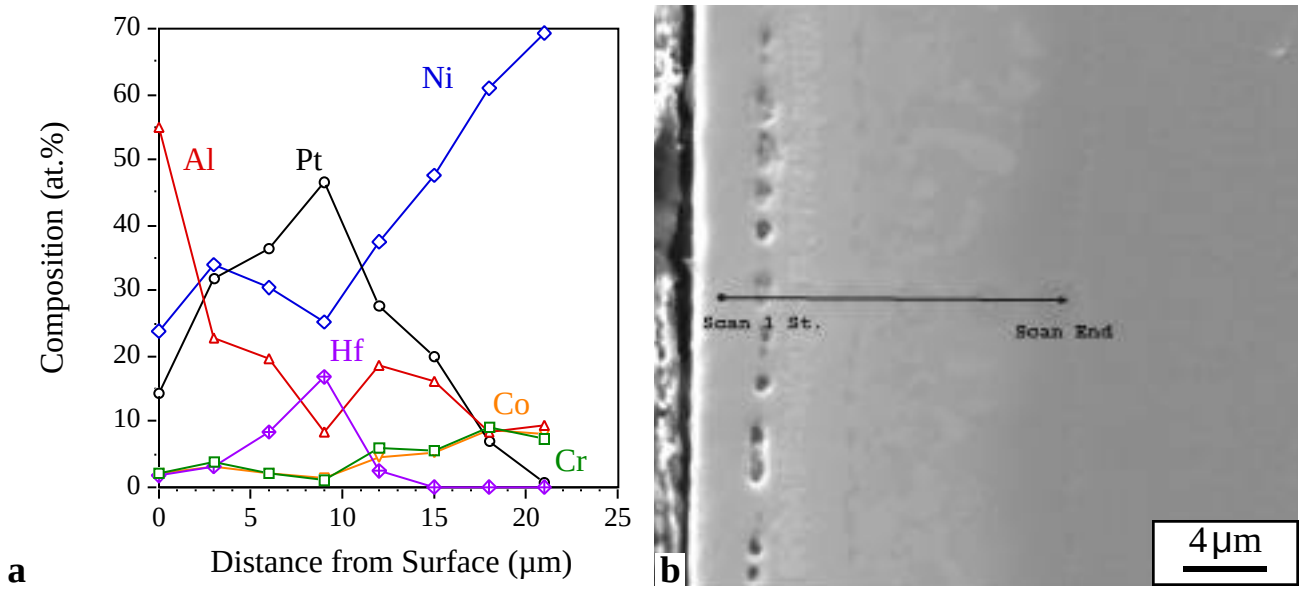

Figure 4. (a) EPMA profile of PHB5 after heat treatment and aluminizing. (b) micrograph of region analyzed.

was concern that this reaction could disrupt the coating. However, heat treatments at 1050° and 1100°C did not show any unusual behavior. Figure 5a shows the cross-section of a specimen with a 5μm Pt/1μm Hf coating after a heat treatment of 2h at 1100°C. A similar layered structure forms but much larger voids were observed after the higher temperature anneal. Figure 5b shows the same specimen after CVD aluminizing for 3h at 1100°C. The Pt-Hf layer is no longer distinctly visible although chemical analysis has not been completed at this time. These preliminary results indicate that higher temperature annealing does not appear to be beneficial.

Status of Milestones

FY 2004
Complete characterization and testing of the first batch of precious metal-based diffusion barriers and report disclosable findings in an open literature publication.
(September 2004)

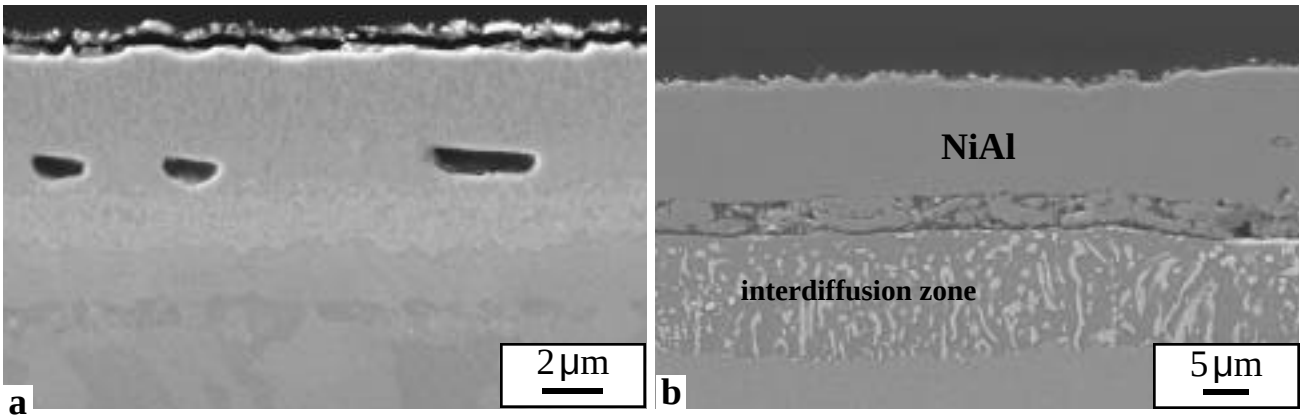

Figure 5. Specimen PHB8 after (a) heat treatment at 500°C for 1h and 1100°C for 2 h, (b) heat treatment plus 3 h CVD aluminizing at 1100°C.

Industry Interactions

Pre-oxidized superalloys were sent to Tom Houvouras of Huntington Plating Inc (Huntington, WV) for Ni-plating of additional pre-oxidized superalloys.

Problems Encountered

None

Publications

None

POWER ELECTRONICS

High Temperature Heat Exchanger

E. Lara-Curzio, J. G. Hemrick, A. Zaltash, N.C. Gallego, C.A. Walls
Metals and Ceramics Division
Oak Ridge National Laboratory
P.O. Box 2008, Oak Ridge, TN 37831-6069
Phone: (865) 574-1749, E-mail: laracurzioe@ornl.gov
B.E. Thompson
University of Western Ontario

Objective

As part of a collaborative effort between ORNL and the University of Western Ontario, graphite-based heat exchangers will be designed and evaluated for heat recovery systems in microturbine applications. In particular, it is desired to improve the efficiency of heat recovery systems based on aluminum fin heat exchangers that are currently being used in commercial units. In coordination with modeling efforts, the microstructure of graphite-based heat exchangers will be designed in order to maximize heat transfer while minimizing pressure drop. The efficiency of the new designs will be compared against currently used aluminum fin heat exchangers and eventually evaluated using a Unifin Microgen heat recovery unit couple to a Capstone C60 microturbine.

Work will be supplemented with experiments to gain a better understanding of the effect of heat exchanger material microstructure on gas flow penetration, pressure drop, and mechanical strength.

Technical Progress

Upon consideration of the costs and labor associated with connection of the Unifin Microgen heat exchanger to the 60 kW Capstone microturbine, discussion was held regarding the feasibility of using the current microturbine/heat exchanger system already in place at the ORNL Cooling, Heating, and Power Facility (bldg. 3115). This option would utilize the already existing infrastructure and instrumentation, while allowing alteration to the current equipment to facilitate the testing of new heat exchanger concepts.

Efforts to fabricate a “miniature wind tunnel” device were combined with expertise at the University of Western Ontario. Carbon foam samples with varying densities were prepared at ORNL and supplied to Materials Resources International for S-bond joining to aluminum plates. These joined samples will be provided to the University of Western Ontario for testing in their existing wind tunnel facility. Information on the depth of gas penetration in these systems is important to optimize material usage.

Development and implementation of a method to evaluate and compare the mechanical properties of individual foam ligaments using X-ray tomography and rapid prototyping techniques has been continued. Low spatial resolution (28μm) CT scans were performed at Argonne National Laboratory. High spatial resolution (3μm) CT scans were performed at the

Japan Fine Ceramics Center in Nagoya, Japan. Estimates are still being sought for file conversion and rapid prototyping services.

High thermal conductivity graphite fiber samples have been obtained. Lower thermal conductivity/lower modulus fiber materials have also been identified and samples have been obtained. A commercial company (3-Tex, Inc. of Cary, NC) has been identified as a partner in the project. They have a unique weaving process (3-Weave) which is capable of producing 3-dimensional fiber preforms. A visit was made to 3-Tex and possible preform weaving techniques and designs were discussed. Out of the meeting, it was decided that a series of preforms would be woven with and without metallic tubing incorporated in the structure. Initial weavings will use 50 msi/lower thermal conductivity fibers. Subsequent weavings will be attempted with higher modulus/higher thermal conductivity fibers. Fiber has been ordered for the initial weavings and production time is being scheduled at the 3-Tex Rutherfordton, NC facility.

Brian Thompson and Qijun Yu, from the University of Western Ontario, visited ORNL in early May. Both presented seminars outlining their work and progress in regard to the modeling of carbon foam and the design of alternative carbon foam heat exchangers. The design of microturbine/heat exchanger experiments, the base-line performance of the current Unifin heat exchanger, and the cooling of power electronics were also discussed.

A test rig has been designed and constructed to evaluate heat transfer, permeability, and pressure drops associated with experimental graphite foams and woven fiber preform structures. Results will be used to optimize the pore structures of foams and fiber preforms to maximize performance and to verify model predictions.

Status of Milestones

In Progress

- Fabrication and joining of samples for wind tunnel analysis at University of Western Ontario. Eight samples have been provided for analysis and additional samples are in preparation (July 2004)
- Alteration of current equipment in place at the ORNL Cooling, Heating, and Power Facility (bldg. 3115) to facilitate the testing of new heat exchanger concepts. (August 2004)
- Development and implementation of a method to evaluate and compare the mechanical properties of individual foam ligaments using X-ray tomography and rapid prototyping techniques. (August 2004)
- Testing of carbon foam and fiber performs in test rig. (August 2004)
- Fabrication of carbon-fiber preform prototypes. (September 2004)

Problems Encountered

None

Publications/Inventions/Meetings

Visit to 3-Tex, Inc., Cary, NC to discuss 3-dimensional weaving process (4/04)

Visit by Brian Thompson and Qijun Yu, from the University of Western Ontario (5/04)

Industrial Interactions

Technical discussions have been held with the following organizations:
Albany International Techniweave Inc.
Cytec Carbon Fibers
Ford Motor Company
Javelin
Nippon Graphite Fibers
3-Tex, Inc.
Unifin

Heat Exchange Concepts Utilizing Porous Carbon Foam

B. E. Thompson and A. G. Straatman
Faculty of Engineering
The University of Western Ontario
London, Ontario, Canada N6G 4K1
Phone: (519)850-2530, E-mail: Thompson@eng.uwo.ca

Objective

There is a need to produce engineering models for design of heat exchangers made from emerging porous carbon-foam materials. Knowledge and understanding of the effects of carbon foam on convective heat transfer is crucial to the development of appropriate engineering approximations for these design models. The overall objective is to explore new ideas for heat-exchanger configurations, especially for situations in which current technology is marginally cost effective. A thermo-economic model and a strategic design study are planned to provide new understanding for assessment in a stage-gate approach to further prototype development.

Highlights

Alternative designs of air-cooled heat exchangers for electronics and of water-cooled for inverters on hybrid electric automobiles have been generated using carbon foam as the primary heat transfer surface. Engineering analysis is being performed to down selecting the most promising configurations. A model of the structure of carbon foam has been formulated in order to calculate physical characteristics of importance to thermal modeling. Comparisons with ORNL measurements are being done to validate the model. The design of experiments to assess the interstitial flow under the porous surface has been completed and the test apparatus is under construction.

Technical Progress

A computational model has been developed both for the pressure drop and heat transfer rate in porous carbon foam because, in part, high heat transfer with minimal pressure drop are the motivations in heat exchanger design. The pressure-drop component of the model was formulated based on the Darcy-Forchheimer equation because of its validity in low to intermediate Reynolds number flows, specifically those in the aforementioned applications. A constant Nusselt number correlation was derived for the prediction of heat transfer coefficients based on slug flow in a channel with one wall at constant temperature and the others adiabatic. The computational modeling approximations required validation and this was done with data taken from experiments performed at Oak Ridge National Laboratory in which a heater was attached to the top of a block of carbon foam that was mounted in a channel in such a way that the fluid passing through the channel was forced convection cooling the foam. Calculations were compared to measured bulk outlet temperatures and pressure drop in the ranges of flow rates from 25

to 45 USgpm and heater power from 300 to 600 W. For test conditions of 25 USgpm and 300 W, the calculated pressure drop was 6.700 kPa and compared a measured value of 6.895 kPa; the measured outlet bulk temperature was about 3% more than predicted, and the calculated and measured temperature distributions across the outlet agreed within 0.8%. For flow rates of 45 USgpm and heater power in the range 300 to 600 W, agreement between measured and calculated pressure drop and outlet bulk temperature were within 12% and 0.5%, with the latter being within experimental uncertainty and perhaps somewhat fortuitous. Although the computational model was developed with simple geometries, it could be applied to complex geometries for design purposes.

Status of Milestones

The next milestones are the validation of the computational model, selection of the most promising heat exchanger concepts made from carbon foam, and the set up of the windtunnel for experiments to quantify heat transfer from the surface of carbon foam.

Industry Interactions

Unifin continues to support Western efforts to obtain better understanding of heat-exchanger performance and selection issues for microturbine applications. Ford Motor Company has interacted with students, of course, while under the supervision of Professor Albert Shih at the University of Michigan.

Problems Encountered

Professor Thompson will relocate to become the Dean of Engineering at the University of Ottawa on July 1st.

Publications/Presentations

Thompson, B.E. and Yu, Q.: Development of an ultra-efficient air to water heat exchanger using carbon foam. DOE/CETC Conference on Microturbine Applications, Los Angeles, CA, January 20-23, 2004.

Hemrick, J. G., Lara-Curzio, E., Zaltash, A., Gallego, N. C., Walls, C. A., Thompson, B. E.: Evaluation and Application of High Thermal Conductivity Materials for Microturbine Heat transfer Systems. DOE/CETC Conference on Microturbine Applications, Los Angeles, CA, January 20-23, 2004.

Yu, Q. and Thompson, B. E: Thermal engineering model of a heat exchanger with finned tubes made from porous carbon foam. CSME Forum 2004, June 1-4, 2004. University of Western Ontario, London, Canada.

MATERIALS FOR ADVANCED RECIPROCATING ENGINES

Spark Plug Erosion and Failure

H. T. Lin and M. P. Brady
Oak Ridge National Laboratory
Oak Ridge, TN 37831-6068
Phone: (865) 576-8857, E-mail: linh@ornl.gov

Objective

This subtask focuses on two parallel efforts. The first task will characterize the electrode near-surface region microstructure in spark plugs before and after engine testing to understand corrosion/erosion mechanisms as a function of engine condition (environment) and time in determining the lifetime limiting processes. The information gained from the first task will feed into an exploratory alloy development effort for electrode materials with improved corrosion/erosion resistance to extend the long-term durability and lifetime performance of spark plugs for advanced reciprocating engines.

Highlights

Setup of a bench type electrode material screening test rig has been completed during this reporting period (Fig. 1). The test rig will provide a cost-effect approach to screening the oxidation/erosion resistance of developmental of alloys. Also, results would provide guidelines for alloy design to improve the oxidation/erosion resistance. The Pt alloy would be used as a reference for comparison.

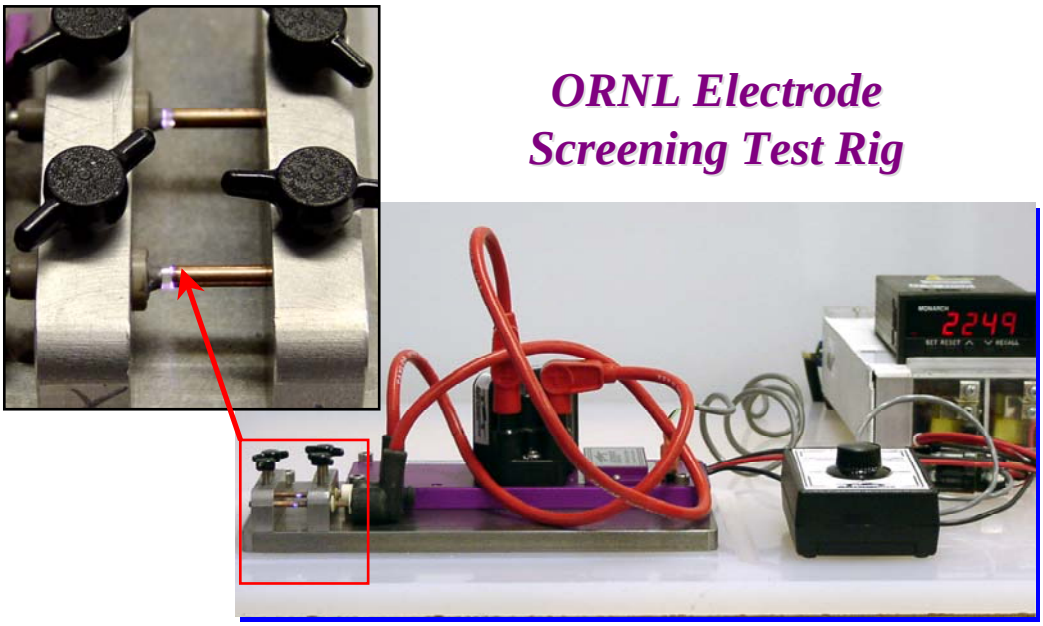

Figure 1. Photo shows the bench type electrode material screening test rig.

Technical Progress

Quantitative compositional analysis was performed on the polished cross-sections of as-received and field-tested spark plugs by electron probe microanalysis (EPMA) using pure element standards. These as-received and field-tested spark plugs with operating times of 4,386h, manufactured by Champion, Federal Mogul Corp., were acquired from Caterpillar Inc. The purpose of these quantitative analyses was to confirm and characterize the size of interdiffusion zone between Ni-base alloy electrode and Pt-W alloy and Ir tip insert if they existed after the joining process. Results of EPMA showed that there existed a significant interdiffusion zone of Pt-W tip insert with the Ni-base electrode (Fig. 2). The size of interdiffusion zone ranged from 250 to 300 µm. On the other hand, no apparent interdiffusion zone was observed between Ni-base electrode and Ir tip insert, as shown in Fig. 3. Note that similar compositional profiles were also obtained for tested plugs. The formation of this interdiffusion zone between Ni-base alloy electrode and Pt-W alloy insert occurred during joining process. The Ni-Pt solid solution zone, which exhibits a high oxidation susceptibility, would readily oxidize at temperatures of 800-1000°C and form Ni-Pt-O compounds. The dominant crack could readily initiate at the interface corner of oxidized interdiffusion zone (Ni-Pt-O), which is brittle in nature, when subjected to thermomechanical stress during operation. Note that an oxidized interdiffusion zone with an extensive crack generation along the interface between Ni alloy electrode and Pt-W tip insert was consistently observed for all tested plugs (Fig. 4). When the crack reached a critical size and completely separated the Pt-W insert from the Ni-base ground electrode, it could have a significant impact on the long-term durability and lifetime of spark plugs.

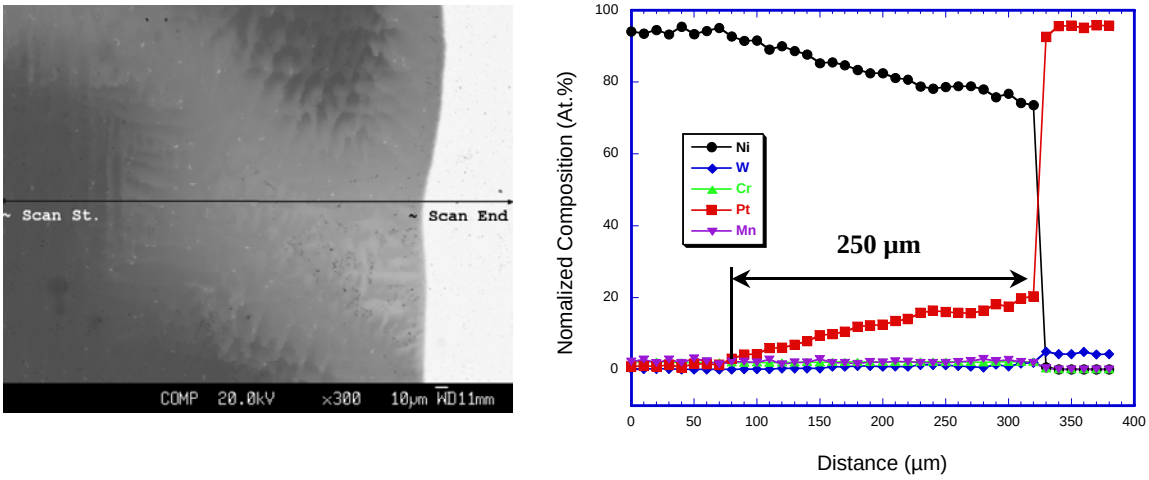

Figure 2. Quantitative compositional profile across the Ni-base electrode and Pt-W alloy tip insert interface.

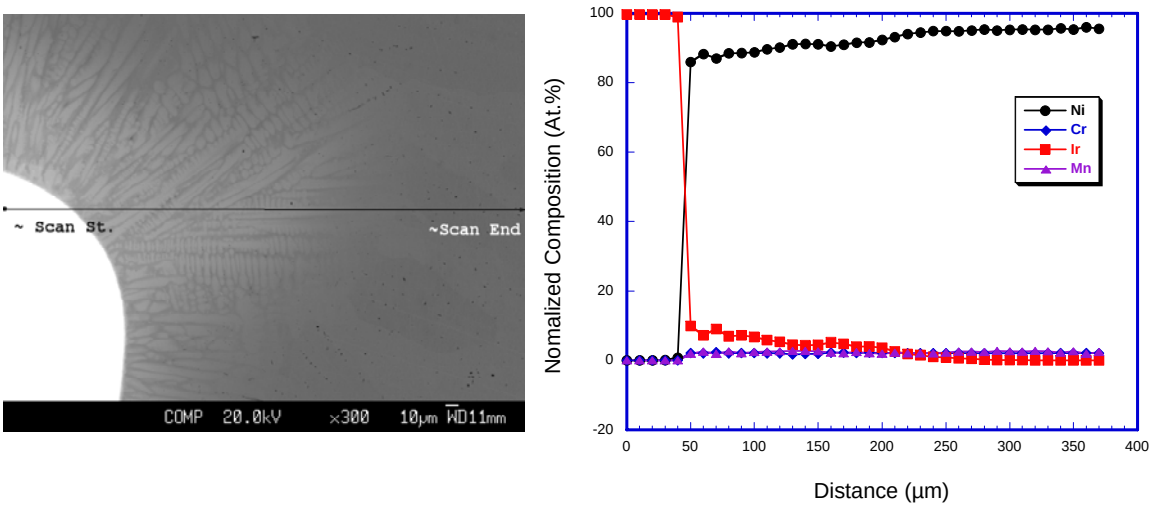

Figure 3. Quantitative compositional profile across the Ni-base electrode and Ir tip insert interface.

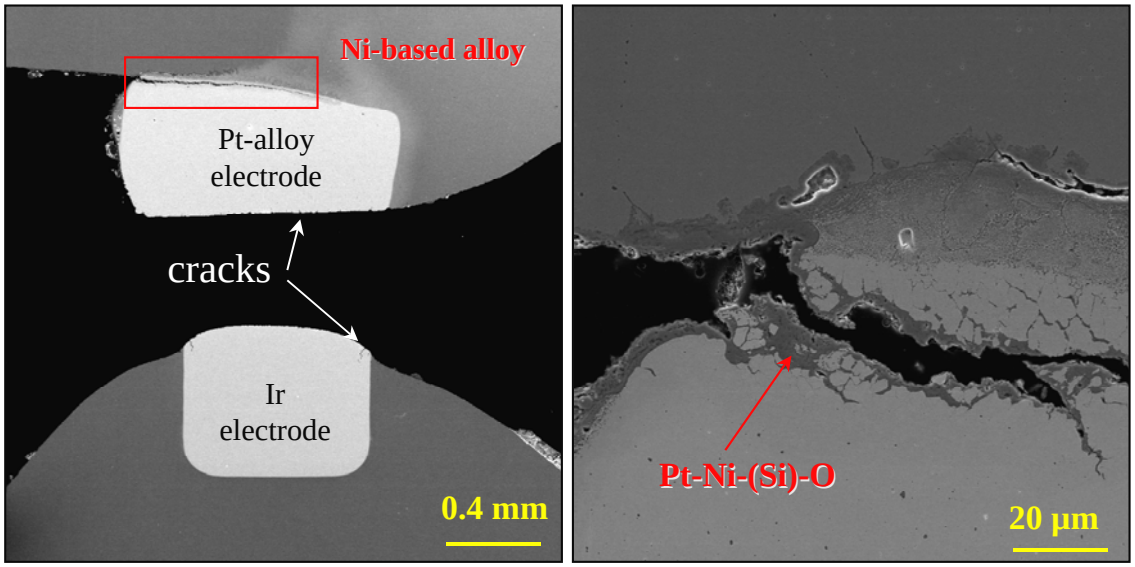

Figure 4. SEM micrographs show an extensive crack generation along the Ni-base alloy electrode and Pt-W ally tip insert after field service.

Based on initial observations of cracking and corrosion issues in the Pt and Ir electrode insert tips from worn natural gas engine spark plugs, two developmental Cr-base alloys were designed and manufactured for testing. These two Cr-base alloys were designed with melting points in excess of 1800°C and oxide additions to improve ductility. The high levels of Cr are expected to impart excellent corrosion resistance, and resist the cracking phenomena observed. The alloys were hot-pressed for consolidation, and then EDM machined to make 1/8" diameter rods for initial evaluation for sparking resistance. This testing will be initiated in the next quarter.

Status of Milestones

Establish test protocol for rapidly screening developmental alloys for resistance to spark erosion and complete initial assessment of 1 material class/protection phenomenon for improved erosion resistance. September 2004. On schedule.

Industry Interactions

Drs. Rangarajan and Derra from Waukesha Engine visited ORNL and NTRC on March 30th to discuss the spark plug and ignition system issues and potential collaborative research area.

Drs. Benson and Tozzi from Woodward visited ORNL and NTRC on March 30th to discuss the ignition system and spark plug issues and potential collaborative research area.

Communication with Caterpillar on the microstructure characterization results for spark plugs after 4,386h field service.

Problems Encountered

None

Publications/Presentations

R. K. Richards, H. T. Lin, and M. P. Brady, "Characterization of Erosion Mechanisms of Natural Gas Engine Spark Plugs" has been submitted for presentation and publication at ASME International Combustion Engine Division, 2004 Fall Technical Conference, Long Beach, CA, October 24-27, 2004.

Advanced Materials for Exhaust Components of Reciprocating Engines

P. J. Maziasz, N. D. Evans, J. J. Truhan, and K. L. More
Metals and Ceramics Division
Oak Ridge National Laboratory
P.O. Box 2008, Oak Ridge, TN 37831-6115
Phone: (865) 574-5082, E-mail: maziaszpj@ornl.gov

Objective

This program is expanding to consider limitations of various critical in-cylinder and exhaust system components due to performance, temperature capability, and tribology for advanced natural gas reciprocating engine systems (ARES). While initial efforts focused on exhaust valves, recent input from engine manufactures has expanded the scope to include intake and exhaust valves and seats, as well as other exhaust components. The program is engaged in active dialog to define the long-term needs and priorities of engine makers.

Highlights

ORNL microcharacterization of a Ni-based superalloy exhaust valve (Pyromet 31V) after moderate engine service was completed last quarter. Engine service produces additional precipitates within grains and along grain boundaries, in addition to coarsening the γ' that hardens the matrix. Fatigue resistance is summarized for a new CF8C-Plus cast austenitic stainless steel, developed for exhaust component applications, that is now being commercialized. New discussions of materials R&D needs began with Waukesha Engine Division, Dresser Industries this quarter, and they visited ORNL at the end of the quarter.

Technical Progress

Microcharacterization of exhaust valves of Pyromet 31V (Ni-22Cr-15Fe alloy with Ti and Al for γ' precipitation hardening), provided by Waukesha Engine Division, Dresser Industries, Inc. was completed last quarter. Microcharacterization of the valves in the middle of the combustion face, comparing fresh and engine tested valves, showed that aging during engine service produced significant changes in microstructure, causing additional precipitation in the matrix and along grain boundaries. The γ ' phase particles that harden the matrix after the initial heat-treatment, coarsen after moderate service at less than 700^{o}C.

Last year, ORNL and Caterpillar developed a new cast austenitic stainless steel, CF8C-Plus, that has the potential for use as exhaust component applications in advanced diesel engines. Typical exhaust manifolds and turbocharger housings are made from SiMo cast iron, which has poor strength above 550-600^{o}C, and can be susceptible to thermal fatigue cracking during severe cycling after prolonged use. Standard CF8C steel (Fe-19Cr-9Ni-

0.7Nb-0.07C), has good castability and sufficient strength up to about 600-625^{o}C, but is not strong enough at higher temperatures. CF8C steel contains a large amount (20-25 vol.%) of δ-ferrite, which then transforms into σ-phase during aging at 600^{o}C and above, and severely reduces ductility. CF8C-Plus steel was developed to be stronger and much more fatigue and thermal fatigue resistant for use in severe thermal cycling conditions. CF8C-Plus has an "engineered microstructure" that contains no δ-ferrite in the as-cast microstructure, and hence no σ-phase forms during aging.

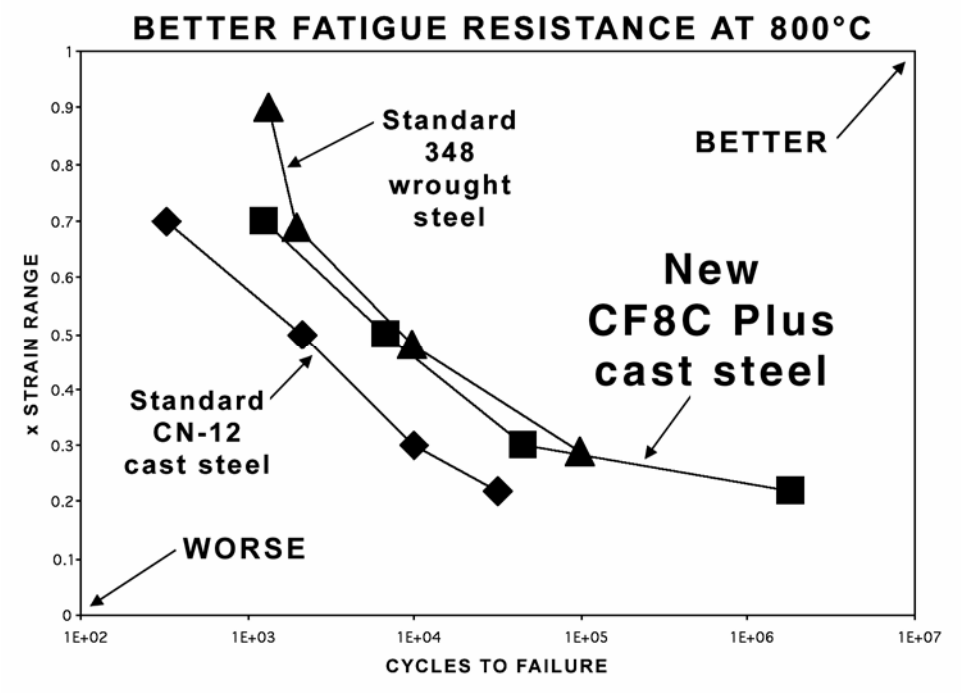

Figure 1. Isothermal fatigue testing of commercial standard CN12 and new CF8C-Plus stainless steels at 800^{o}C. The CF8C-Plus has significantly better fatigue cracking resistance than standard CN12 steel, and both are much better than SiMo cast iron at these conditions.

The isothermal fatigue resistance of a new commercial heat of the CF8C-Plus steel at 800^{o}C is much better than standard, commercial CN-12 steel (Fig. 1). Both stainless steels are much better than SiMo cast iron at these conditions. The new CF8C-Plus steel is currently being commercialized, and may be applicable for exhaust components of advanced ARES engines.

This quarter discussions began with Waukesha Engine Division to expand the materials needs for in-cylinder and exhaust component applications. Discussions included valve seats and guides as well as valves for both intake and exhaust valves, and included bulk metallurgical properties as well as surface behavior (corrosion, tribology). The discussions led to a visit by Waukesha managers to ORNL at the end of the quarter (March 30, 2004).

Status of Milestones

FY 2004 – Complete characterization Ni-based superalloy (Pyromet 31V) valves to define aging effect during engine service. Define aging effects at weld overlay and coating bond regions (December 2003) – completed.

Industry Interactions

New discussions with Waukesha Engine Dresser, Inc. (Jim Drees, Joe Derra, Roger Rangarajan, and others) about materials needs and interests for advanced ARES engines with ORNL (Tom King, Tim Theiss, Phil Maziasz and John Truhan) began this quarter, and will continue next quarter.

Problems Encountered

None

Publications/Presentations

None

Development of Catalytically Selective Electrodes for NOx and Ammonia Sensors

T. Armstrong, F. Montgomery, and D. West
Oak Ridge National Laboratory
P.O. Box 2008, Oak Ridge, TN 37831-6084
Phone: (865) 574-7996, E-mail: armstrongt@ornl.gov

Objective

To develop non-catalytic and catalytically selective electrodes for use in NOx and ammonia sensors and to build and test sensors using the materials and technology developed

Technical Highlights (NO Selective Sensor Development)

1. New electrode geometries investigated this quarter (use two materials, same number as "original" design).
2. NO response (w/o bias) tends to be stronger than "original design", although still much less than NO_2 response.
3. Semicircular and interdigitated geometries appear to offer enhanced recovery time (in mixed-potential mode) when compared to original design (operating without bias).
4. Response/recovery time not a strong function of geometry for semicircular and interdigitated geometries.
5. New element geometries (semicircular and interdigitated) exhibited "NO-selective" behavior when current biased.

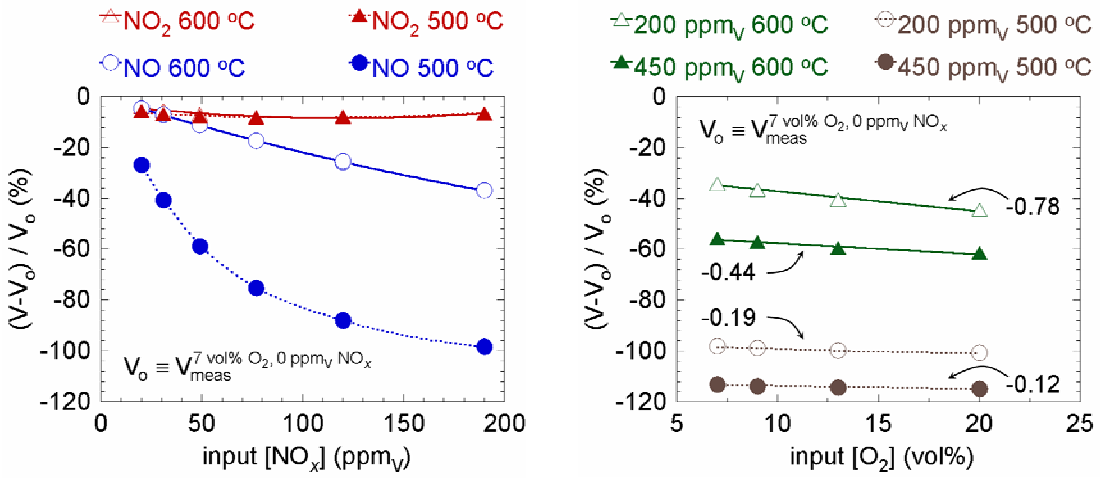

Figure 1. NO_x sensing performance of the semicircular element with current bias. For the graph on the right, the input NO_x was NO and the numbers are the slope of a linear fit to $(V-V_o) / V_o$ vs. $[O_2]$.

Status of Milestones

1. Determine kinetics of NO reaction on electrode as a function of temperature and environment.
   This is ongoing and will continue as new electrode materials are developed and tested as well as new sensor designs.

2. Fabricate and test a prototype NOx sensor (09/03)
   We are focusing on refining the NO and total NOx sensors. Testing of these sensors is ongoing.

Communications/Visits/Travel

Cummings has expressed interest in our program and discussions are being initiated to brief them on our progress.

Problems Encountered

None

Publications

Electrically Biased NO_x Sensing Elements with Co-Planar,Multi-Layered Electrodes submitted to Journal of the Electrochemical Society.

Presentations

Electrically Biased NO_x Sensing Elements with Co-Planar, Multi-Layered Electrodes presented at the Electrochemical Society Meeting, San Antonio, TX May 2004.

Internal Distribution

B. L. Armstrong, 4515, MS-6063, armstrongbl@ornl.gov
T. R. Armstrong, 4508, MS-6084, armstrongt@ornl.gov
P. F. Becher, 4515, MS-6068, becherpf@ornl.gov
T. M. Besmann, 4515, MS-6063, besmanntm@ornl.gov
C. A. Blue, 4508, MS-6083, blueca@ornl.gov
M. P. Brady, 4500S, MS-6115, bradymp@ornl.gov
M. A. Brown, 4500N, MS-6186, brownma@ornl.gov
M. K. Ferber, 4515, MS-6069, ferbermk@ornl.gov
J. A. Haynes, 4515, MS-6063, haynesa@ornl.gov
D. R. Johnson, 4515, MS-6066, johnsondr@ornl.gov
M. A. Karnitz, 4500N, MS-6186, karnitzma@ornl.gov
J. O. Kiggans, 4508, MS-6087, kiggansjojr@ornl.gov
T. J. King, 4515, MS-6065, kingtjjr@ornl.gov
J. W. Klett, 4508, MS-6087, klettjw@ornl.gov
E. Lara-Curzio, 4515, MS-6069, laracurzioe@ornl.gov
H. T. Lin, 4515, MS-6068, linh@ornl.gov
R. A. Lowden, 4515, MS-6063, lowdenra@ornl.gov
P. J. Maziasz, 4500S, MS-6115, maziaszpj@ornl.gov
K. L. More, 4515, MS-6064, morekl1@ornl.gov
R. D. Ott, 4515, MS-6083, ottr@ornl.gov
S. D. Nunn, 4508, MS-6087, nunnsd@ornl.gov
B. A. Pint, 4500S, MS-6156, pintba@ornl.gov
D. T. Rizy, 3147, MS-6070, rizydt@ornl.gov
D. P. Stinton, 4515, MS-6063, stintondp@ornl.gov
R. W. Swindeman, 4500S, MS-6155, swindemanrw@ornl.gov
T. N. Tiegs, 4508, MS-6087, tiegstn@ornl.gov
P. F. Tortorelli, 4500S, MS-6156, tortorellipf@ornl.gov
I. G. Wright, 4500S, MS-6157, wrightig@ornl.gov
A. Zaltash, 3147, MS-6070, zaltasha@ornl.gov

External Distribution

ALLISON ADVANCED DEVELOPMENT CO., 1100 Wilson Blvd., Suite 1450, Arlington, VA 22209
J. Miles, r.jeffrey.miles@allison.com

ALM SYSTEMS, INC, 1920 N Street, NW, Suite 750, Washington, DC 20036
M. Kalin, mkalin@ibek.com

ARGONNE NATIONAL LABORATORY, 9700 S. Cass Ave., Argonne, IL 60439-4838
W. Ellingson, ellingson@anl.gov
J. P. Singh, jpsingh@anl.gov

BATTELLE MEMORIAL INSTITUTE, 505 King Avenue, Columbus, OH 43201
D. Anson, ansond@battelle.org

BAYSIDE MATERIALS TECHNOLOGY, 21150 New Hampshire Ave., Brookville, MD 20833
D. Freitag, dfreitag@ix.netcom.com

BCS, INC., 5550 Sterrett Place, Suite 216, Columbia, MD 21044
D. Bartley, dbartley@bcs-hq.com

BOWMAN POWER, 20501 Ventura Boulevard #285, Woodland Hills, CA 91364
T. Davies, tdavies@bowmanpower.co.uk
T. Hynes, ahynes.bowmanpower@att.net
D. Flaxington, dflaxington@bowmanpower.co.uk

CALIFORNIA ENERGY COMMISSION
A. Soinski, asoinski@energy.state.ca.us

CANNON-MUSKEGON CORP., Box 506, Muskegon, MI 49443-0506
J. Wahl, jwahl@canmkg.com

CAPSTONE TURBINE CORP., 6430 Independence Ave., Woodland Hills, CA 91367
P. Chancellor, pchancellor@capstoneturbine.com
K. Duggan, kduggan@capstoneturbine.com
M. Stewart, mstewart@capstoneturbine.com
J. Willis, jwillis@capstoneturbine.com
M. Rodrigues, mrodrigues@capstoneturbine.com
B. Treece, btreece@capstoneturbine.com

CERAMATEC INC., 2425 South 900 West, Salt Lake City, UT 84119
C. Lewinsohn, clewinsohn@ceramatec.com
B. Nair, bnair@ceramatec.com

CLEMSON UNIVERSITY, South Carolina Institute for Energy Studies, 386-2, Clemson, SC 29634-5180
L. Golan, glawren@clemson.edu
R. Wenglarz, rwnglrz@clemson.edu
J. Hinson, jhinson@clemson.edu

CONNECTICUT RESERVE TECHNOLOGIES, 2997 Sussex Ct., Stow, OH 44224
E. Baker, baker@crtechnologies.com
S. Duffy, sduffy@crtechnologies.com
J. Palko, jpalko@crtechnologies.com

DTE ENERGY, 37849 Interchange Dr., Suite 100, Farmington Hills, MI 48335
M. Davis, davism@dteenergy.com

ELECTRIC POWER RESEARCH INSTITUTE, 3412 Hillview Ave., Palo Alto, CA 94303
J. Stringer, jstringe@epri.com

ELGILOY SPECIALTY METALS, 1565 Fleetwood Drive, Elgin, IL 60123

T. Bartel, terryb@elgiloy.com

ELLIOTT ENERGY SYSTEMS, 2901 S.E. Monroe Street, Stuart, FL 34997
D. Burnham, dburnham@elliott-turbo.com
D. Dewis, ddewis@elliott-turbo.com

ENERGETICS, INC., 501 School St., SW, Suite 500, Washington, DC 20024
R. Scheer, rscheer@energeticsinc.com

ENERGY TECHNOLOGIES APPLICATIONS, 5064 Camino Vista Lujo, San Diego, CA 92130-2849
T. Bornemisza, borneger@ix.netcom.com

GAS TURBINE ASSOCIATION, 1050 Thomas Jefferson St., NW, 5th Fl, Washington, DC 20007
J. Abboud, abboud@advocatesinc.com

GENERAL ELECTRIC (GE) CR&D, 1 Research Circle, Building K1-RM 3B4, Niskayuna, NY 12309
S. Correa, correa@crd.ge.com
K. Luthra, luthra@crd.ge.com
M. VanDerwerken, vanderwerken@crd.ge.com
C. Johnson, johnsonca@crd.ge.com

GENERAL ELECTRIC AIRCRAFT ENGINES, One Neumann Way, Mail Drop M89, Cincinnati, OH 45215-1988
R. Darolia, ram.darolia@ae.ge.com

GENERAL ELECTRIC POWER SYSTEMS, One River Rd., 55-127, Schenectady, NY 12345
R. Orenstein, robert.orenstein@ps.ge.com

GENERAL ELECTRIC POWER SYSTEMS, Gas Technology Center, 300 Garlington Road, Greenville, SC 29615
P. Monaghan, philip.monagham@ps.ge.com

HAYNES INTERNATIONAL, INC., 1020 W. Park Avenue, P.O. Box 9013, Kokomo, IN 46904-9013
V. Ishwar, vishwar@haynesintl.com
D. Klarstrom, dklarstrom@haynesintl.com

HONEYWELL CERAMIC COMPONENTS, 2525 W. 190th St., Torrance, CA 90504
D. Foley, dan.foley@honeywell.com
C. Li, chien-wei.li@honeywell.com
D. Newson, danielle.newson@honeywell.com
M. Savitz, MaxineSavitz@aol.com
J. Wimmer, jim.wimmer@honeywell.com
M. Mitchell, michele.mitchell@honeywell.com

HONEYWELL COMPOSITES, 1300 Marrows Rd., PO Box 9559, Newark, DE 19714-9559
L. Connelly, liz.connolly@ps.ge.com
P. Gray, paul1.gray@ps.ge.com
D. Landini, dennis.landini@ps.ge.com

HONEYWELL ENGINES, SYSTEMS, & SERVICES 2739 E. Washington St., PO Box 5227, Phoenix, AZ 85010
B. Schenk, bjoern.schenk@honeywell.com
HONEYWELL POWER SYSTEMS, 8725 Pan American Freeway NE, Albuquerque, NM 87113
S. Wright, e.scott.wright@honeywell.com

HOWMET RESEARCH CORP., 1500 South Warner St., Operhall Research Center, Whitehall, MI 49461-1895
B. Mueller, bmueller@howmet.com
R. Thompson, rthompson@howmet.com

INGERSOLL-RAND ENERGY SYSTEMS, 32 Exeter St., Portsmouth, NH 03801
A. Kaplau-Colan, alex_haplau-colan@ingersoll-rand.com
M. Krieger, michael_krieger@irco.com
J. Johnson, jay_johnson@ingersoll-rand.com
J. Kesseli, jim_kesseli@ingersoll-rand.com
J. Nash, jim_nash@ingersoll-rand.com

KENNAMETAL INC. 1600 Technology Way, P.O. Box 231, Latrobe, PA 15650-0231
R. Yeckley, Russ.yeckley@kennametal.com

KINECTRICS NORTH AMERICA, 124 Balch Springs Circle, SW, Leesburg, VA 20175
B. Morrison, blake.Morrison@kinectrics.com

KRUPP VDM TECHNOLOGIES CORP., 11210 Steeplecrest, Suite #120, Houston, TX 77065-4939
D. Agarwal, dcagarwal@pdq.net

NASA GLENN RESEARCH CENTER, 21000 Brookpark Rd., MS 49-7, Cleveland, OH 44135
D. Brewer, david.n.brewer@grc.nasa.gov
J. Gykenyesi, john.p.gyekenyesi@lerc.nasa.gov
S. Levine, stanley.r.levine@lerc.nasa.gov
N. Nemeth, noel.n.nemeth@grc.nasa.gov
B. Opila, opila@grc.nasa.gov

NATIONAL RURAL ELECTRIC COOPERATIVE ASSOC., 4301 Wilson Blvd., SS9-204, Arlington, VA 22203-1860
E. Torrero, ed.torrero@nreca.org

NATURAL RESOURCES CANADA, 1 Haanel Drive, Nepean, Ontario, Canada K1A 1M1
R. Brandon, rbrandon@nrcan.gc.ca

PCC AIRFOILS, INC., 25201 Chagrin Blvd., Suite 290, Beachwood, OH 44122
C. Kortovich, ckortovich@pccairfoils.com

PENN STATE UNIVERSITY, Applied Research Laboratory, PO Box 30, State College, PA 16823
J. Singh, jxs46@psu.edu

RICHERSON AND ASSOC., 2093 E. Delmont Dr., Salt Lake City, UT 84117
D. Richerson, richersond@aol.com

ROLLS-ROYCE ALLISON, 2925 W. Minnesota St., PO Box 420, Indianapolis, IN 46241
S. Berenyi, steve.g.berenyi@allison.com
P. Heitman, peter.w.heitman@allison.com
F. Macri, francis.g.macri@allison.com
J. Oswald, jim.oswald@rolls-royce.com

SAINT-GOBAIN CERAMICS & PLASTICS, INC., Goddard Road, Northboro, MA 01532
B. LaCourse, Brian.C.LaCourse@saint-gobain.com
R. Licht, robert.h.licht@saint-gobain.com
M. Abouaf, Marc.Abouaf@saint-gobain.com
V. Pujari, Vimal.K.Pujari@saint-gobain.com
A. Vartabedian, Ara.M.Vartabedian@saint-gobain.com

SEBESTYEN, T., Consultant, 6550 Mission Ridge, Traverse City, MI 49686-6123
T. Sebestyen, sebestyen@chartermi.net

SIEMENS WESTINGHOUSE POWER CORP., 1310 Beulah Rd., Pittsburgh, PA 15235-5098
M. Burke, michael.burke@swpc.siemens.com
C. Forbes, christian.forbes@swpc.siemens.com

SOLAR TURBINES, INC., TurboFab Facility, 16504 DeZavala Rd., Channelview, TX 77530
B. Harkins, harkins_bruce_d@solarturbines.com

SOLAR TURBINES INC., 818 Connecticut Ave., NW, Suite 600, Washington, DC 20006-2702
R. Brent, solardc@bellatlantic.net

SOLAR TURBINES, INC., 2200 Pacific Highway, PO Box 85376, MZ R, San Diego, CA 92186-5376
P. Browning, browning_paul_f@solarturbines.com
M. Fitzpatrick, fitzpatrick_mike_d@solarturbines.com
P. Montague, montague_preston_j@solarturbines.com
M Van Roode, van_roode_mark_x@solarturbines.com
M. Ward, ward_mike_e@solarturbines.com
J. Price, jeffprice@solarturbines.com

SOUTHERN CALIFORNIA EDISON COMPANY, 2244 Walnut Grove Avenue, Rosemead, CA 91770

S. Hamilton, hamiltsl@sce.com

SOUTHERN COMPANY, 600 N. 18th Street, 14N-8195, P.O. Box 2641, Birmingham, AL 35291

S. Wilson

STEVEN I. FREEDMAN, Engineering Consultant, 410 Carlisle Ave., Deerfield, IL 60015

S. Freedman, sifreedman@aol.com

STAMBLER ASSOCIATES, 205 South Beverly Drive, Suite 208, Beverly Hills, California 90212

I. Stambler

THE BOEING COMPANY, Rocketdyne Propulsion & Power, 6633 Canoga Avenue
MC: GB-19, P.O. Box 7922, Canoga Park, CA 91309-7922

G. Pelletier, gerard.pelletier@west.boeing.com

TELEDYNE CONTINENTAL MOTORS, 1330 W. Laskey Rd., PO Box 6971, Toledo, OH 43612-0971

J. T. Exley, texley@teledyne.com

TURBEC

L. Malmrup, lars.malmrup@turbec.com

UCI COMBUSTION LABORATORY, U. of CA, Irvine, Irvine, CA 92697-3550

V. McDonell, mcdonell@ucic1.uci.edu

UDRI, Ceramic & Glass Laboratories, 300 College Park Ave., Dayton, OH 45469-0172

A. Crasto, allan.crasto@udri.udayton.edu
G. Graves, gravesga@udri.udayton.edu
N. Osborne, osborne@udri.udayton.edu
R. Wills, roger.wills@udri.udayton.edu

UNITED TECHNOLOGIES RESEARCH CENTER, 411 Silver Lane MS 129-24, East Hartford, CT 06108

H. Eaton, eatonhe@utrc.utc.com
J. Holowczak, holowcje@utrc.utc.com
T. Rosfjord, rosfjotj@utrc.utc.com
J. Smeggil, smeggijg@utrc.utc.com
G. Linsey, linseygd@utrc.utc.com
J. Shi, shij@utrc.utc.com
E. Sun, suney@utrc.utc.com
D. Mosher, mosherda@utrc.utc.com

UNIVERSITY OF CALIFORNIA, Department of Mechanical Engineering, Berkeley, CA 94720
R. Dibble, rdibble@newton.berkeley.edu

UNIVERSITY OF COLORADO, Department of Mechanical Engineering, Boulder, CO 80309-0427
R. Raj, rishi.raj@Colorado.edu

UNIVERSITY OF MARYLAND, Department of Mechanical Engineering, College Park, MD 20742-3035
R. Radermacher, rader@eng.umd.edu

UNIVERSITY OF WESTERN ONTARIO, Faculty of Engineering, London, Ontario, Canada N6G 4K1
B. E. Thompson, Thompson@eng.uwo.ca
A. G. Straatman, astraat@engga.uwo.ca

US DOE-NETL, P. O. Box 880, MSO-D01, 3610 Collins Ferry Rd., Morgantown, WV 26507-0880
C. Alsup, Jr., charles.alsup@netl.doe.gov
A. Layne, abbie.layne@netl.doe.gov
L. Wilson, lane.wilson@netl.doe.gov

US DOE-NETL, PO Box 10940, Pittsburgh, PA 15236
N. Holcombe, norman.holcombe@netl.doe.gov
U. Rao, rao@netl.doe.gov

US DOE CHICAGO OPERATIONS OFFICE, 9800 S. Cass Ave., Argonne, IL 60439
J. Jonkouski, jill.jonkouski@ch.doe.gov
J. Mavec, joseph.mavec@ch.doe.gov
J. Livengood, joanna.livengood@ch.doe.gov
S. Waslo, stephen.waslo@ch.doe.gov

US DOE-HQ, 1000 Independence Ave., S.W., Washington DC 20585
R. Fiskum, ronald.fiskum@ee.doe.gov
D. Haught, debbie.haught@ee.doe.gov
P. Hoffman, patricia.hoffman@ee.doe.gov
W. Parks, william.parks@ee.doe.gov
M. Smith, merrill.smith@ee.doe.gov
C. Sorrell, charles.sorrell@ee.doe.gov

WILLIAMS INTERNATIONAL, 2280 West Maple Rd., PO Box 200, Walled Lake, MI 48390-0200
G. Cruzen, g.cruzen@williams-int.com
W. Fohey, w.fohey@williams-int.com
C. Schiller, cschiller@williams-int.com

WRIGHT PATTERSON AIRFORCE BASE,

R. Sikorski, ruth.sikorski@wpafb.af.mil